ARTICLE

Deposit-scale structural architecture of the Sigma-Lamaque gold deposit, Canada—insights from a newly proposed 3D method for assessing structural controls from drill hole data

E. J. Cowan [1,2]

Abstract

Deposit-scale structural analysis is a practical method of structurally analyzing 3D drilling data. This interpretation method uses readily available distributed 3D data at the most relevant scale for mining and exploration. This method does not depend on collecting traditional structural data from core, such as orientation of planar and linear data, but relies on the premise that grade distributions sampled from drilling provide insight into the structural control of the deposit, with the interpretation of structural geometry done using a computer 3D viewer. This method is applied to the well-studied Archean Sigma-Lamaque gold deposit, which features late-orogenic vein mineralization, and which is controlled by three orders of structural features. The first-order control is the easterly plunging pipe-like conduit parallel to F_2 fold plunge defined by the intersection of bedding (S_0) and foliation (S_2) (~ 1.5 km radius × 3 km down-plunge). The second-order controls, nested within the first-order, are the younger subvertical Late Diorite plugs that intruded vertically into the host rocks along the established S_2 foliation anisotropy (1250:400:150 m dimension for Main Plug). The third-order control, laterally limited by first- and second-order structural controls, is the well-documented gold-bearing vein sets (1–10 m thick and up to 1.5 km in extent) that developed in the Late Diorites and in the older folded volcanogenic stratigraphy and diorites. It is proposed that the first-order control defined by the moderately plunging F_2 fold is the main fluid pathway resulting from structural permeability formed during earlier folding. The second-order Late Diorite plugs and other competent lithological units, which intersected and fractured during late-stage D_2 compression, served as chemically reactive sites causing gold to precipitate along this first-order pathway. It is predicted that intrusions that do not intersect the first-order structural conduits are less likely to be mineralized. Greenfield orogenic-gold exploration requires that the first-order controls are identified, and the geometry of hydrothermal alteration is best understood in the context of the structural architecture of the host rocks.

✉ E. J. Cowan
jun@juncowan.com

1 JunCowan, PO BOX 230, Fremantle 6959, WA, Australia

2 School of Earth, Atmosphere and Environment, Monash University, Clayton 3800, VIC, Australia

Introduction

Drill data are the best three-dimensional (3D) dataset the mineral industry has access to.

Despite the historical limitations of unsophisticated data—most databases contain only a single column of data for a single element (e.g., Au), and many are also under-sampled with many sample gaps—the drilling database is still best for studying mineral deposits. But, scant attention is given to the deposit-scale 3D patterns that can be gleaned from these deposit-wide data, yet the structural patterns gleaned from these data at the deposit-scale can guide further exploration in the surrounding region.

🖄 Springer

Using historical drilling and mined stope data, the Sigma-Lamaque gold deposit is used as a case study for a new approach to examine mineralization patterns. This approach allows sophisticated deposit-scale analysis of the structural patterns within the data to be conducted from single element and lithology table data; that is, data lacking traditional structural measurements (such as orientations of planar and linear data) but commonly available for most mineral deposits. By applying this evaluation method to other ore bodies, where only unsophisticated historical data are available, exploration opportunities can be assessed in 3D, thereby opening up new opportunities for exploration in close proximity to existing deposits.

This study also offers a new structural perspective on the Sigma gold deposit (one half of the Sigma-Lamaque deposit and already extensively studied), which is interpreted as a shear zone-hosted orogenic gold deposit (Robert and Brown 1986a, b; Sibson et al. 1988). This shear zone-hosted interpretation has been used as a template to interpret numerous gold deposits around the world.

The practical importance of deposit-scale structural analysis

Like many industries, the mineral industry is currently in the midst of a data-driven revolution. Substantial increases in drilling activities have resulted in the rapid sampling and delineation of mineral deposits in 3D. The ability to obtain previously unobtainable data from drill cores (e.g., high-precision multi element data, hyperspectral data, X-ray tomography and fluorescence, topography scans) has increased exponentially over the last two decades, and this trend is likely to continue (Haest et al. 2012a,b; Schodlok et al. 2016; Arne et al. 2016; Sjöqvist et al. 2017; Bergqvist et al. 2019). Implied in the collection of such multiple datasets, and the ability to computationally process this information, is an assumption that there will be a direct translation into better understanding of ore deposits, increased identification of near-mine exploration targets, and increased confidence in Resource estimations.

Despite this increase in capacity and technical capability, massive write-downs of Resources and Reserves in structurally controlled gold deposits continue. Despite the large amounts of drill sampling examples of these problems include the Phoenix gold mine in Canada in 2016 (Financial Post 2016) and more recently in Guyana (Financial Post 2019). How can these Resource write-downs occur when mining operations claim to efficiently obtain abundant drilling data to minimize the risk associated with Resource estimation? Could a fundamental geological knowledge gap be the cause of these write-downs?

One critical knowledge gap may be the cause: the study of the structural control of mineral deposits at the deposit scale.

"Deposit-scale" refers to observations that can be made from the entire drill sampling, with or without modeled Resource wireframes. Traditionally, and reflecting limited access to the deposit and its the drill hole database, structural controls have been determined on subsets of a deposit then scaled-up. This practice applies to most academic studies and many studies commissioned by companies.

Deposit-scale structural analysis is a simple, rapid, and practical approach to mineral deposit analysis that focuses on the structural analysis of drilling data at the scale of the mineral deposit. These data are usually single element ± logged lithology data. Importantly, they are not reliant on structural data obtained from the core or outcrop. As introduced in this study, this approach contrasts with typical published mineral-deposit analysis, which rarely examine the geometric patterns at the mineral deposit scale.

The traditional exploration workflow of mineral deposit analysis at a regional scale focuses mainly on regional 2D datasets (e.g., aeromagnetic, gravity, soil geochemistry). These are interpreted to establish the tectonic setting and are followed by field work to obtain outcrop, core, and micro-scale observations (note: "Outcrop" is a general term describing macroscopic scale, which includes stope-scale that applies to underground mines). Geochemical analyses of hand samples provide information about primary and alteration mineral assemblages. All these 2D datasets are commonly analyzed in the context of a published theoretical ore deposit or structural model (Vearncombe and Zelic 2015), and an interpretation is made to explain and predict the origin of the mineral deposit(s).

Discussion of the observed geometric nature of the deposit at the deposit scale in 3D, and its likely structural controls, is conspicuously absent in most mineral deposit research articles and deposit descriptions (e.g., Phillips 2017). This is despite nearly all mining and exploration companies having 3D wireframes of their ore deposits at their disposal. These took time to meticulously digitize in serial sections or which they constructed rapidly using 3D interpolation (Cowan et al. 2002, 2003). In the mining industry, these Resource wireframes are treated as merely shapes: practical containers in which various commodities are estimated using geostatistical procedures. However, very few studies ascribe geological meaning to the 3D distribution of mineralization. Even if geological meaning is assigned to grade distribution, the traditional workflow uses indirect observations and interpretations (largely from micro- to meso-scale, but not directly from observed patterns at the deposit-scale) to infer the deposit-scale patterns and controls (Fig. 1). The 3D wireframes of a Resource are rarely explained in terms of geological patterns or controls that are recorded by geologists at other scales (Fig. 1).

Historically, analytical tools were developed to analyze structural patterns at all scales except the deposit scale, which is "siloed" from being considered as a structural geological
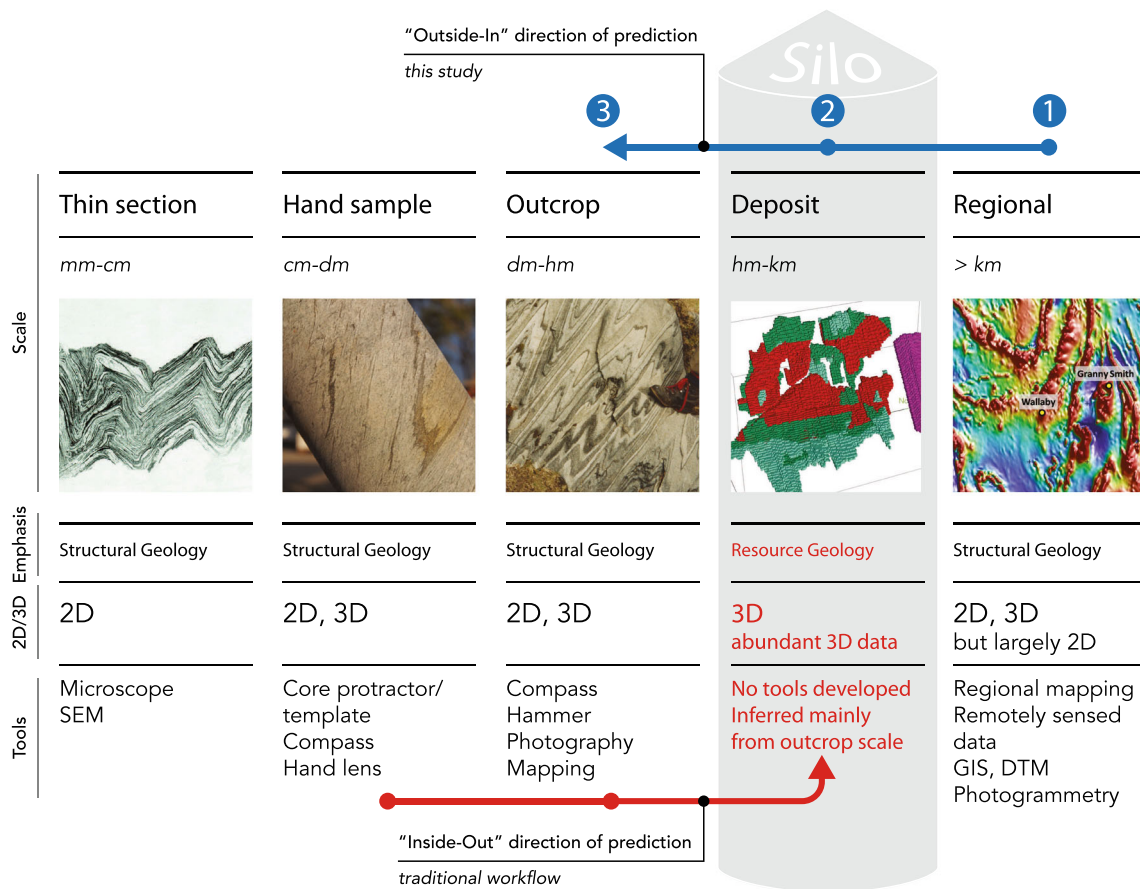
Fig. 1 Scales of observation and associated tools of investigation of mineral deposits. No specific tools have been developed to study structural patterns at the deposit scale

problem. Instead, deposit-scale analysis is considered a Resource definition problem and is largely ignored in applied structural analysis (Fig. 1). Traditionally, structural controls at the deposit scale are predicted from outcrop and hand sample scales, with interpretation occurring along the "Inside-Out" direction shown by the red arrow in Fig. 1. This practice of inferring large-scale geological patterns from the small scale, assuming scale-invariant relationships across a range of scales, is known as the Pumpelly's Principle (Pumpelly et al. 1894; Van Hise 1896). In contrast, this study advocates an "Outside-In" analytical approach for interpreting structural features from a larger scale, which is more reliable because predictions can be made, and field tested. Deposit-scale patterns are predicted inward from regional 3D data, and outcrop-scale patterns are predicted inward from deposit scale (1 to 2 then 2 to 3 along the blue arrow in Fig. 1).

In this study, the main benefits of deposit-scale structural analysis are highlighted by discussing a classic orogenic gold deposit—the Sigma-Lamaque gold deposit in Quebec, Canada, that has been the subject of many decades of highly influential studies, beginning with François Robert's seminal work (1983). This example of deposit-scale structural analysis shows how simple and powerful this "Outside-In" method is to decipher

the structural controls of the mineral deposit and answer many issues that were not addressed by previous research on this deposit, all of which focused on up-scaling outcrop observations.

The Sigma-Lamaque gold deposit

Background

The Lamaque and Sigma deposits (discovered by surface prospecting in 1924 and 1933, respectively) were the first discoveries in the Val-d'Or region of Quebec, Canada (Fig. 2) and became the region's largest gold producers (Poirier et al. 2015a). When operational (1935–1985), the Lamaque mine produced approximately 24 million tonnes of ore, grading 5.9 g/t gold for a total of 4.6 million ounces of gold, and for a time it was the largest gold producer in Quebec. The Sigma mine (operational 1937–1997) produced approximately 24 million tonnes of ore, grading 5.8 g/t gold for a total of 4.5 million ounces of gold. Minor production continued at both mines intermittently from 1997 to 2012. From 1935 to 2012, the combined production from the Sigma and Lamaque mines was approximately 55.9 million tonnes of ore, grading
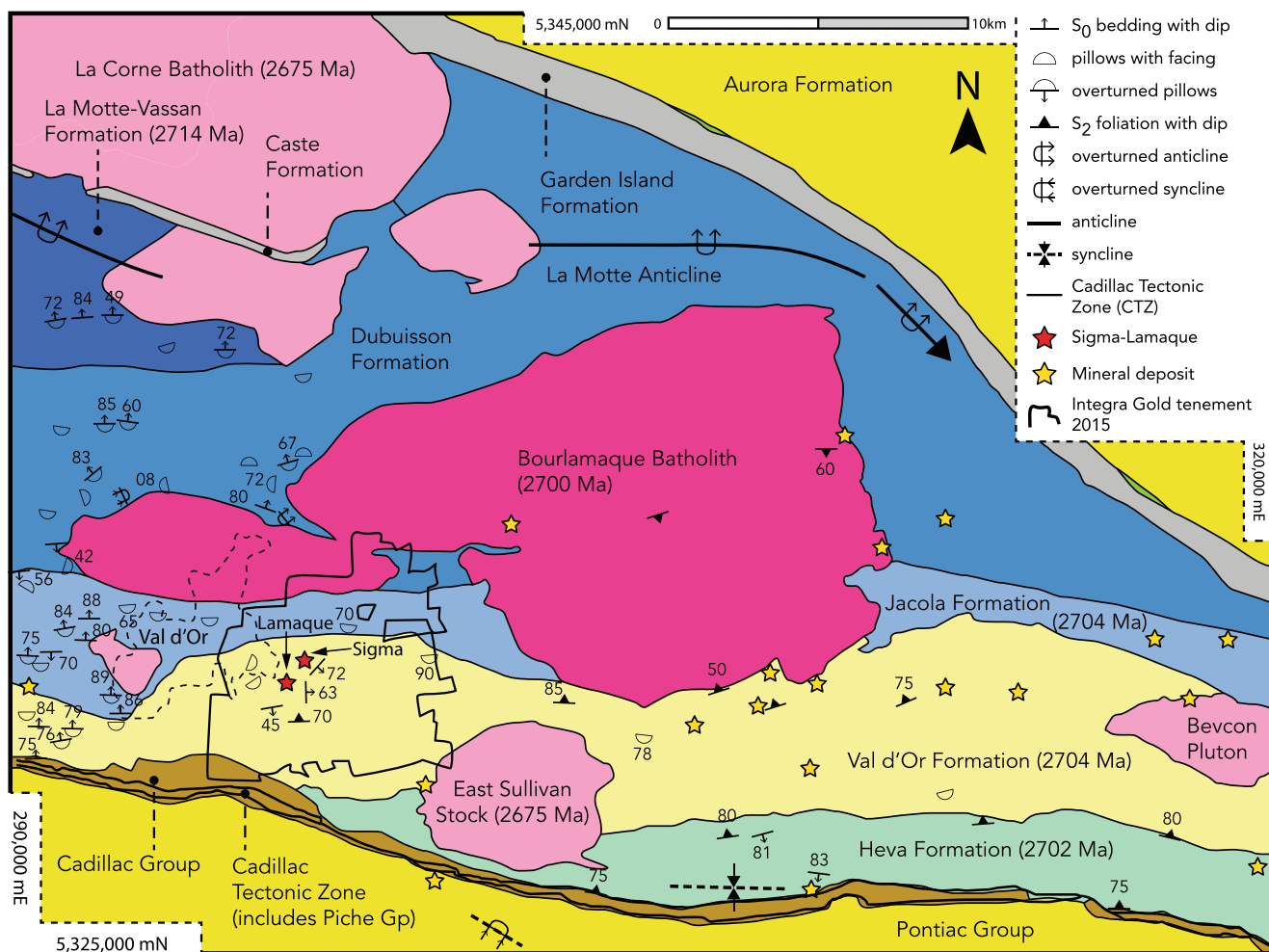
Fig. 2 A synthesis of the regional geologic setting of the Sigma-Lamaque gold deposit in the Val-d'Or camp, southern Abitibi Subprovince, Quebec. Geology compiled from Imreh (1982), Robert (1989), Desrochers and Hubert (1996), Tremblay (2001), and Scott et al. (2002). See Fig. 3 for geochronological references and ± age ranges. Red stars show the Sigma (north) and Lamaque (south) mines. The city of Val-d'Or is located at 48.098709°, − 77.796768° and UTM Zone 18U

5.3 g/t gold for 9.5 million ounces of gold, which is more than half the historic production of the Val-d'Or mining camp and makes the two deposits world-class (Poirier et al. 2015a).

In 2003, Integra Gold Corp acquired the Lamaque South property, south of and adjacent to the Sigma-Lamaque mines (Fig. 2). Mineral Resource estimates and preliminary economic assessment studies followed (Poirier et al. 2015a, b), and, late in 2014, Integra Gold acquired the Sigma-Lamaque mines. Eldorado Gold Corporation subsequently acquired the property from Integra Gold in 2017, and commenced commercial production in March, 2019.

The study presented here was conducted in late 2015 as one of the submissions to the public *Integra Gold Rush Challenge* competition (Integra Gold Corp 2015), which was modeled on the *Goldcorp Challenge* crowdsource competition held in 2000 (Wilde and Kreuzer 2016). For the competition, Integra Gold released its entire geological and drilling databases, including wireframes of modeled ore bodies and stope shapes; the drilling database was cleaned by Integra Gold to remove errors and inconsistencies. This data contained more than 35,000 surveyed holes, comprising 700,000 assay and 170,000 lithology logs. Of these thousands of holes, only 77 were assessed in this study to have data integrity issues and they were omitted from the analysis.

Geological setting

The Sigma-Lamaque gold deposit (previously referred to as two separate deposits) is located in the eastern segment of the southern volcanic zone of the Archean Abitibi Subprovince, immediately north of the boundary with the Pontiac Subprovince (Fig. 2). The gold deposit is part of the Cadillac tectonic zone, a 250 km long east–west trending high-strain zone in eastern Ontario and western Quebec (Robert 1989). The Cadillac tectonic zone, which is the boundary between the two subprovinces, is interpreted as a

steep northerly dipping high-strain suture between the two subprovinces and is one of the greatest gold belts on Earth with a current Resource of about 130 million ounces of gold (Rafini 2014). The geology of the Val-d'Or district has been described in detail by previous workers and their articles contain a more complete discussion of the regional geology (Robert 1989; Desrochers and Hubert 1996; Scott et al. 2002; Olivo et al. 2006; Bedeaux et al. 2017). This section only summarizes the geology relevant to the discussion of the deposit-scale controls of Sigma-Lamaque gold mineralization.

The Val-d'Or district comprises a sequence of volcano-sedimentary and intrusive rocks that were emplaced from 2714 to 2611 Ma (Fig. 2). The Jacola Formation contains pillowed and massive tholeiitic basalts, intercalated with komatiites, and it interfingers with the Val-d'Or Formation to the south, which comprises discontinuous and interstratified massive to pillowed lavas and volcaniclastic andesite, dacite, and rhyolite. The Jacola and Val-d'Or Formations are intruded by felsic to mafic bodies that are grouped into three age groups: 2700 Ma synvolcanic Bourlamaque Batholith; the 2680 Ma syn- to late-D_2 diorite/granodiorite intrusions (Jemielita et al. 1989), and 2675 to 2611 Ma late- to post-tectonic intrusions (East Sullivan Stock, La Corne Batholith, and Bevcon Pluton). Most of the high-grade gold mineralization at Lamaque is hosted in the fractured 2680 Ma "Late Diorites," also referred to as the "Main Plug" because of its prolate intrusion geometry (i.e., pencil-shaped but with an elliptical cross-section [Burrows and Spooner 1989]). The bulk of the remaining lower-grade gold mineralization is hosted within the Jacola and Val-d'Or Formations in various intraformational lithologies (Fig. 2).

Structural architecture at multiple scales

Primary volcanic features in both the Jacola and Val-d'Or Formations indicate a younging direction to the south, with the bedding steeply dipping variously to the south-south-east and east within the Sigma-Lamaque tenement south of the Bourlamaque batholith (Robert and Brown 1986a). The bedding strike trajectory trace is S-shaped and mimics the S-shaped trace of the contact boundary of the Jacola and Val-d'Or Formations to the west under the city of Val-d'Or (fig. 4 in Desrochers and Hubert 1996) (Fig. 2). All rock units older than the post-tectonic intrusions (Fig. 2) record ductile and brittle strain that is the result of D_2 deformation. D_1 deformation is localized closer to the Cadillac tectonic zone (Robert 1989) and west of the city of Val-d'Or and does not affect the rocks in the study area (Desrochers and Hubert 1996). The Jacola and Val-d'Or Formations are pervasively foliated at various intensities by S_2 foliation formed during D_2, and measurements of S_2 within the tenement and surrounding area consistently strike east–west and, on average, dip steeply to the north, very similar to the steep inferred northerly dip of the Cadillac tectonic zone (Fig. 2). The level of ductile strain, reflected in the S_2 intensity, increases southward towards the Cadillac tectonic zone (Robert 1989). The main schistosity in the study area is labeled as S_2 and follows the convention adopted in the literature published prior to Bedeaux et al. (2017).

To determine the chronological relationship of the lithologies at Sigma-Lamaque, the major lithological units available as logged units were grouped and ordered by relative age. These units were then matched with the geological units in the chronological chart compiled from Morasse et al. (1995) and Scott et al. (2002) and references cited in these papers (Fig. 3).

The drilling data are divided into the Sigma and Lamaque deposits and the volume for geological modeling was defined (Fig. 4). The boundary between the two volumes is not defined by the two separate mining operations: instead, the planar northerly-dipping boundary is within the low-grade zone and trends parallel to the pervasive S_2 foliation recorded in the host rocks of the Jacola and Val-d'Or Formations. An implicit modeling software (Leapfrog Mining version 2.4.5.17) was used to model the geological units, but this was conducted after the structural geological architecture was determined from raw data by applying the "Outside-In" interpretation process summarized in Fig. 1.

Regional-scale observations

The regional-scale geological map of Val-d'Or and the surrounding district (Fig. 2) was compiled from previously published research (Imreh 1982; Robert 1989; Desrochers and Hubert 1996; Tremblay 2001; Scott et al. 2002), including the most recent geological survey mapping (Pilote 2015a, b).

The regional geological relationships relevant to the Sigma-Lamaque deposit are:

- The Sigma-Lamaque deposit is located on the southern limb of the ESE-plunging overturned La Motte Anticline.
- S_2 readings from the Sigma-Lamaque site are very sparse. However, the literature indicates that S_2 has an approximate dip-azimuth range of 000° to 015° and a dip range of 70° to 90° (Morasse et al. 1995; Scott et al. 2002; Bedeaux et al. 2017), making it axial planar to the La Motte Anticline.
- The bedding readings in the Val-d'Or Formation vary, dipping steeply south as well as being overturned and dipping north; this is consistent with an overturned southern limb of the La Motte Anticline (Fig. 2).
- All younging directions within the Val-d'Or Formation and the underlying Jacola Formation are consistently south (Fig. 2), and younging reversals are only found in
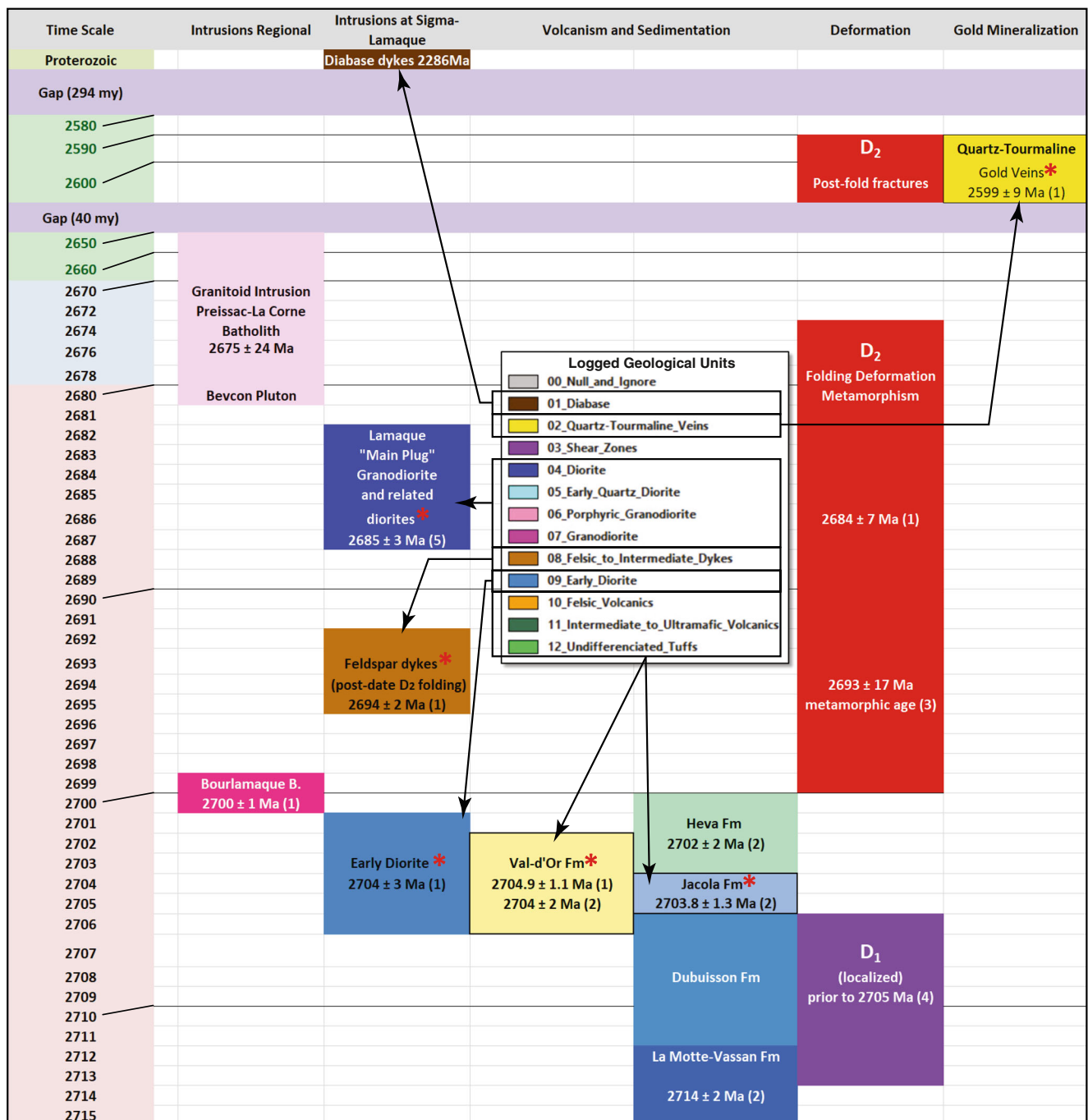
Fig. 3 The Sigma-Lamaque logged drill-hole rock units in descending relative age (inset) in relation to the isotopic ages of the corresponding regional geological units. The oldest three logged units (Felsic Volcanic; Intermediate to Ultramafic Volcanic; Undifferentiated Tuff) are a mixture of the Val-d'Or and Jacola Formations. Sources for age dates are numbered (1) Wong et al. (1991); (2) Scott et al. (2002); (3) Hanes et al. (1989); (4) Desrochers and Hubert (1996); (5) Jemielita et al. (1989), and the mineralized units considered within the Sigma-Lamaque tenement are indicated with a red *

the Heva Formation. This is consistent with the Val-d'Or Formation being located on a limb of a large fold.

- The lower contact of the Val-d'Or Formation with the Jacola Formation is documented as being gradational (Scott et al. 2002). However, the change in strike of this

contact west of Sigma-Lamaque suggests local parasitic folding of this interface (Fig. 2).

- Very few bedding readings are available from the Sigma-Lamaque site. Desrochers and Hubert (1996) suggest the bedding strike changes to mimic the lower contact of the Val-d'Or Formation (Fig. 2); again, this is consistent with

Fig. 4 **a** Plan. **b** Cutaway oblique views of fixed-distance from drilling volumes at Sigma (gray) and Lamaque (yellow). The internal red volume is within 20 m of all drilling and infrastructure. The geological model constructed is constrained to 300 m as indicated. The green volume extends to the tenement boundary, which is indicated in Fig. 2
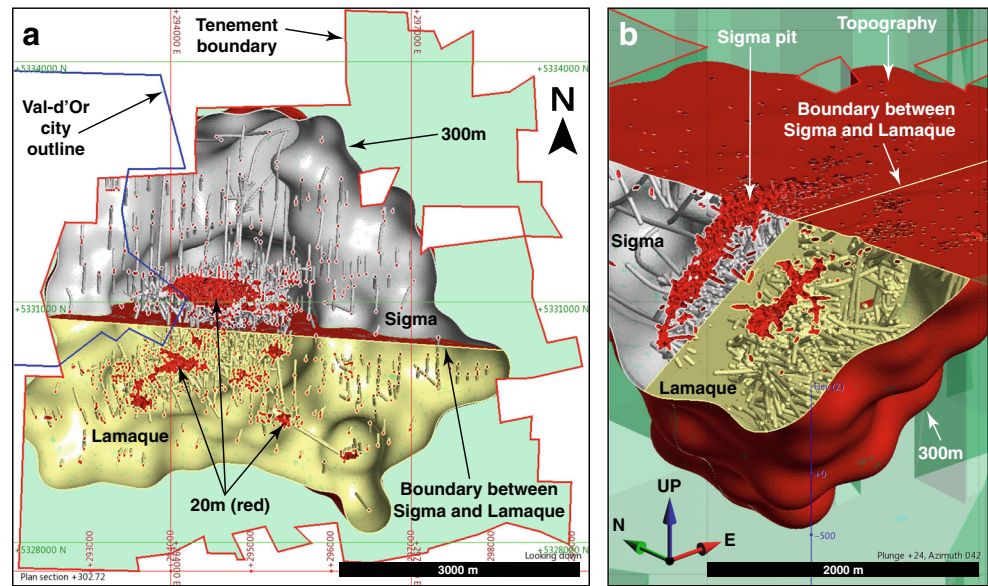
an ESE-plunging parasitic fold ("Val-d'Or Domain" in fig. 5 of Desrochers and Hubert 1996).

- The tightness of the folding is uncertain. The consistently documented (Scott et al. 2002) southerly-facing stratigraphy from the Val-d'Or Formation suggests open folding but Robert and Brown (1986a) and Robert and Poulsen (1997) have indicated isoclinal folding.

Deposit-scale observations

Despite the extensive geological work conducted at the Sigma-Lamaque deposit (Perrault et al. 1984; Robert and Brown 1986a, b; Boullier and Robert 1992; Gaboury et al. 2001; Garofalo et al. 2002; Garofalo 2004; Olivo et al. 2006), many geological peculiarities and features that are recorded at the deposit-scale are not addressed by previous work. The Sigma and Lamaque gold occurrences are only 500 m apart, separated by a northerly-dipping low-grade zone (Fig. 4). Although they are considered a single deposit because of their shared geological history, one of their most striking features is how dissimilar they are in terms of host rock characteristics and deposit geometry.

Key observations, which provide important clues to the geologic control of the gold deposit recorded at the deposit-scale, are listed below.

Observation 1: gold occurrence and lithology are dissimilar at Sigma and Lamaque

There are significant differences in the two deposits between gold occurrence and host lithological units (Fig. 5). The highest mean gold grades are associated with the "Late

Diorite" phases that occur as plugs in the Lamaque area: "Late Diorite" refers to the phases of diorite logged as Diorite, Early Quartz Diorite, Porphyritic Granodiorite, and Granodiorite (Figs. 5 and 6), which are also referred to as the "Main Plug" (Burrows and Spooner 1989).

Gold data separated into Sigma and Lamaque volumes (Fig. 5) show that the Late Diorite plug intrusions are highly mineralized at Lamaque, but are largely absent at Sigma. Conversely, the relatively poorly-mineralized lithological units at Lamaque are the highly mineralized lithological units at Sigma (e.g., Early Diorite, Felsic to Intermediate Dykes) (Fig. 5).

The quartz-tourmaline veins, which carry the high grades right across the Sigma-Lamaque deposit, are late-stage brittle fractures that cross-cut all units (Fig. 3). Early Diorite and Late Diorite plugs are associated with the highest grades and are present at both locations. These relationships suggest that the gold mineralization is not entirely influenced by lithology.

Observation 2: Late Diorite plugs only exist at Lamaque

Although some minor dykes are logged as the Late Diorite phase, characteristic plug-like (prolate, or pencil-shaped) geometries are absent at Sigma. The very linear and steeply plunging Late Diorite plugs are only present in the Lamaque area—this puzzling detail requires geological explanation.

Observation 3: the Late Diorite plugs exhibit preferred orientation and geometry

The geometry and significance of the Lamaque Late Diorite plugs have not been discussed by previous workers despite their importance as hosts of the Lamaque gold mineralization.
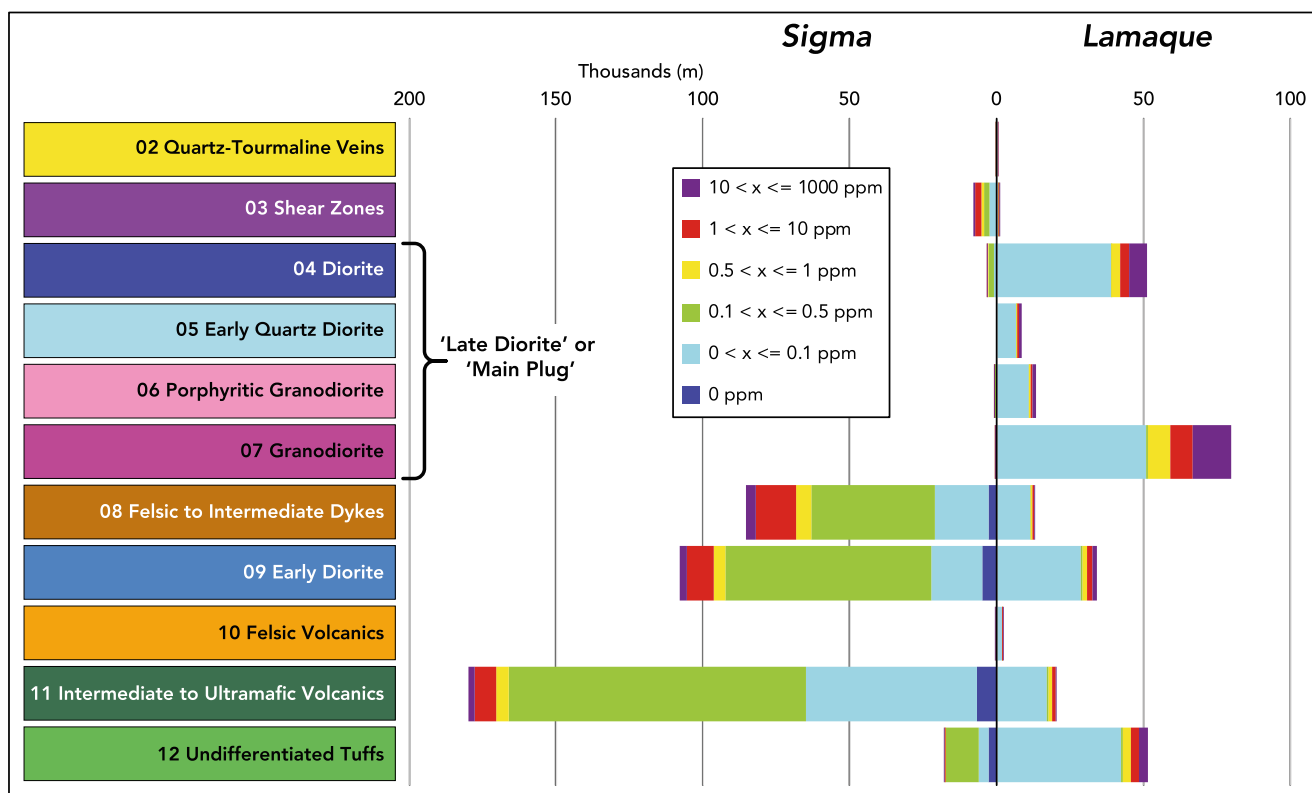
Fig. 5 Relative gold abundance in the Sigma (left) and Lamaque (right) domains in terms of lithological units. The horizontal scale is expressed in summed meters, therefore proportional to the volume of sampling

The Late Diorite plugs exhibit a preferred orientation and are very linear, with the Main Plug at Lamaque plunging towards $76° \rightarrow 026°$. The main mineralized plug is elongate but is triaxial in shape and not perfectly linear with axial lengths $a{:}b{:}c$ of 1250:400:150 m (Fig. 6), and the high-grade gold distribution mimics this overall geometry. The a–b plane defines a planar orientation dipping steeply to the north (Fig. 6d) with an approximately ellipsoidal axial ratio of 8:3:1, which is a prolate geometry according to k-value of 1.3 computed from these axial ratios (Flinn 1962). Although Flinn (1962) developed the k-value measure as a technique to document marker geometries in ductile-strained rocks, this technique is also a convenient way to classify overall shapes of geological units and 3D grade distributions (where $k > 1$ is prolate [pencil shape]; $k < 1$ is oblate [pancake shape]; and $k = 1$ is equally prolate and oblate). The Lamaque intrusions have a peculiar geometry and it would be of interest if this geometry is related to the structural architecture of the Jacola and Val-d'Or Formations that can be deciphered at the deposit-scale.

Observation 4: vein orientations at Lamaque and Sigma display contrasting vein distributions

Sigma and Lamaque sites contain vein-hosted gold mineralization comprising multiple quartz-tourmaline vein sets with variable orientations (Wilson 1948; Robert and Brown 1986a). Using an implicit drawing tool (Cowan et al. 2004), vein orientations for both Sigma and Lamaque were summarized by digitizing the median surfaces of the mined stopes, which correspond with mineralized veins (Fig. 7a), then by plotting all poles of the triangulation faces of the drawn vein median surfaces (Fig. 7b).

Light-blue shading in the stereonets of Fig. 7b shows a departure from perfect cylindricity, and veins at both locations are close enough to be considered a result of plane-strain deformation (i.e., 2D strain). Figure 7b plots the theoretical shear planes and assumes a conjugate vein symmetry relative to the extension veins. Gray shading shows the estimated theoretical compression fields assuming perfect symmetry of thrust shear veins relative to the extension vein orientation (poles of veins, which are extension structures, are not expected to plot in the compression field). The compression field at Lamaque has an angle of 70° and although asymmetric in development, is represented by both north- and south-dipping veins in the extensional field (these are interpreted as thrust shear veins). The compression field at Sigma has an angle of 75°, but the symmetrical low-angle south-dipping shear vein is missing in the extensional field (position of green pole in Fig. 7b for Sigma); instead, as documented by Robert and Brown (1986a), it is replaced by steep south-dipping misoriented reverse shear
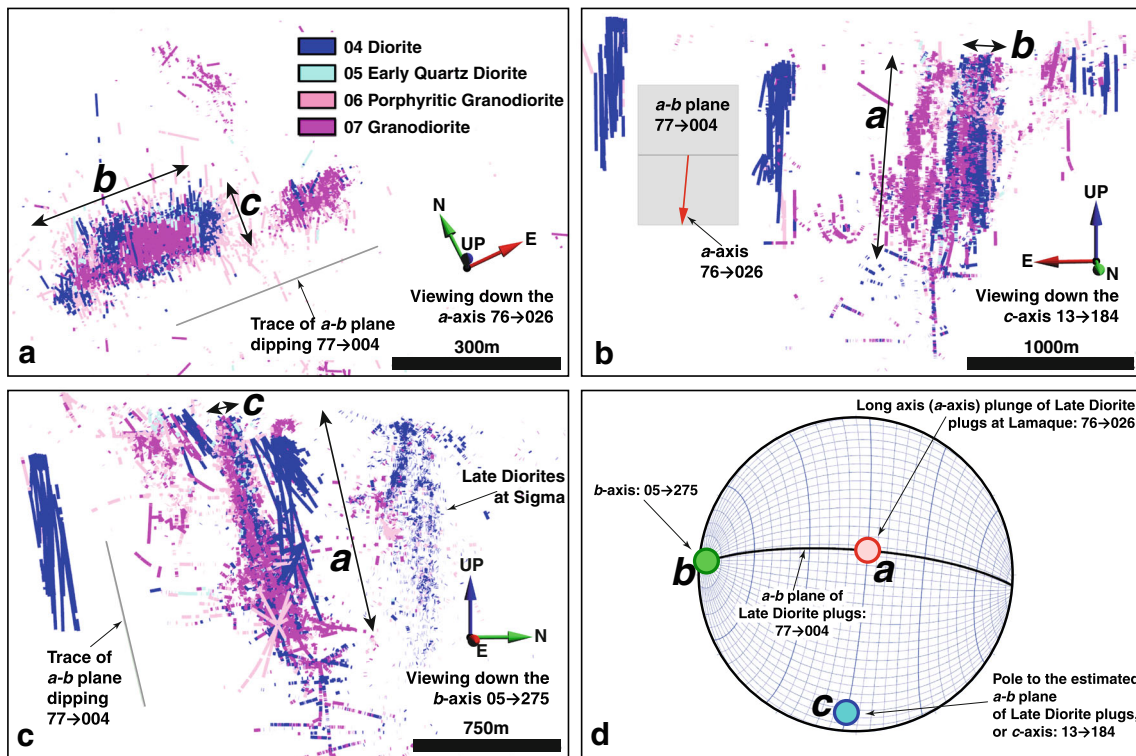
Fig. 6 Geometry and orientation of the Late Diorite plugs at Lamaque. Only the intervals of Late Diorite phases are shown (Diorite, Granodiorite, Porphyritic Granodiorite, and Early Quartz Diorite) (Figs. 3 and 5). The *a*, *b*, and *c* axes are the *Max:Int:Min* axes of the intrusion geometries. **a** View down the long axis of the plug (top 700 m is only shown for clarity). **b** View along the short *c*-axis of the plugs (Late Diorite at Sigma are not shown for clarity). **c** View parallel to the intermediate *b*-axis (the Late Diorites of Sigma on the right are tabular dyke-like intrusions and not strongly linear but still display a linear subvertical long-axial orientation). **d** Axial orientation of the plugs define an *a–b* plane that dips 77° → 004° with a steep *a*-axis plunging 76° → 026°

Fig. 7 Analysis of mineralized veins from Sigma-Lamaque gold deposit. **a** Cross-eyed stereo view of the mineralized vein tangent planes shown as disks (from Lamaque) created for this study by digitizing the median plane of stopes (yellow) combined with grade continuities seen in drilling (not shown). **b** Stereo plots of all vein tangent poles obtained from Sigma and Lamaque areas
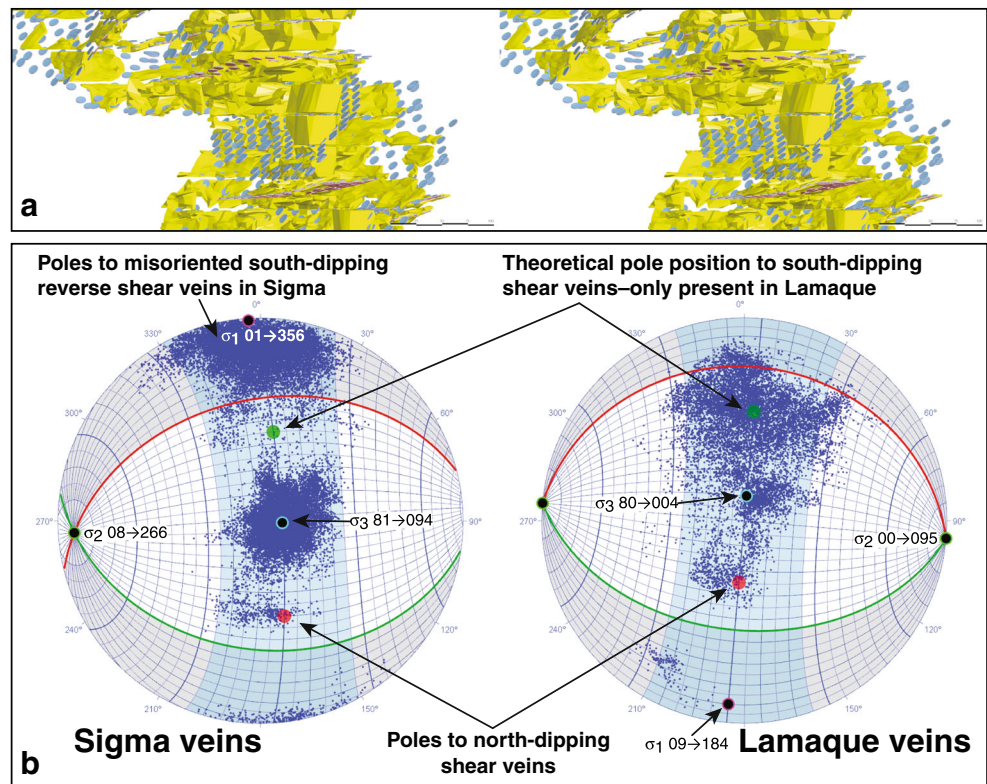
veins (i.e., "misoriented" meaning they are unfavorably oriented for slip and dilation relative to the compression direction determined by the extension veins Sibson [1992]). Bulk strain inferred from the veins developed at Sigma and Lamaque suggests vertical extension and subhorizontal N–S shortening (Fig. 7b). However, no explanation has been documented as to why the sets of vein orientations in the two areas differ markedly in symmetry and orientation. The complete contrast in vein orientations at Sigma and Lamaque, which resulted from the same N–S shortening event, requires a geological explanation because the two areas are only 500 m apart.

Observation 5: the Sigma-Lamaque vein swarms appear to converge at depth

The enveloping surface of the Sigma deposit vein swarm, comprising both shear and extension veins, is subvertical and strikes 260°, whereas the enveloping shape of the Lamaque deposit strikes 274° and dips to the north at an angle of 77°—an angular difference of 19° between the two zones. Although the strike of the deposits is similar, because of this obliquity in dip values, both mineralization zones appear to converge at depth in a V-shaped geometry; however, the zone of apparent convergence is below the current drilling depth. No geological explanation has been put forward to explain this convergence.

Observation 6: the Sigma veins shift orientation systematically with position

At Sigma, the orientations of the veins shift with geographic position. This is particularly evident in the flat extensional veins when viewed towards the north (Fig. 8). The uppermost eastern veins are flat, whereas the westernmost and deeper veins exhibit a low-angle westerly dip (Fig. 8). Although there is a similar degree of orientation shift in the south-dipping shear veins, there has been no geological explanation for these gradual spatial shifts in vein orientations.

Observation 7: an easterly plunging western grade boundary exists at both Sigma and Lamaque

A feature of both Sigma and Lamaque is a 45° easterly-plunging boundary towards the western side of the gold-bearing vein swarms (Fig. 9). No geological control has been proposed for this mineralization limit at the Sigma-Lamaque deposit.

In the next section, a structural geological model for the Sigma-Lamaque deposit is presented that explains all these deposit-scale issues.

Synthesis

The annotated local geological map of Sigma-Lamaque shows an obliquity between first-order bedding (S_0) and S_2 foliation traces (Fig. 10a). Other geological maps of this area show a similar bedding-to-foliation angular relationship, which
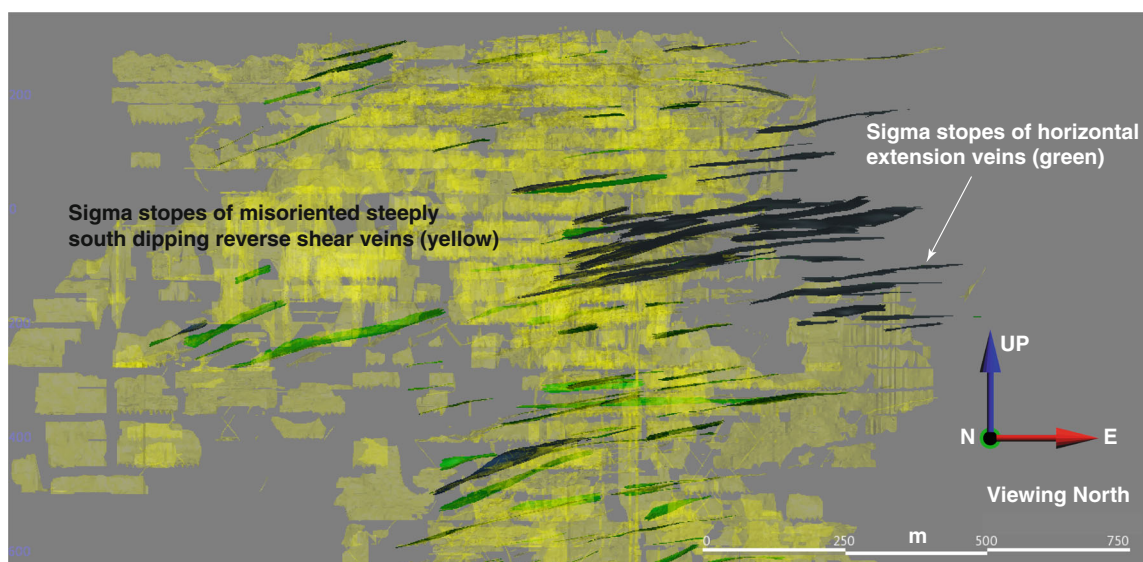

Fig. 8 The stopes of Sigma horizontal veins (green) exhibit a systematic change to higher dips in the westerly direction. The position of this view relative to the entire Sigma gold distribution is shown in Fig. 9
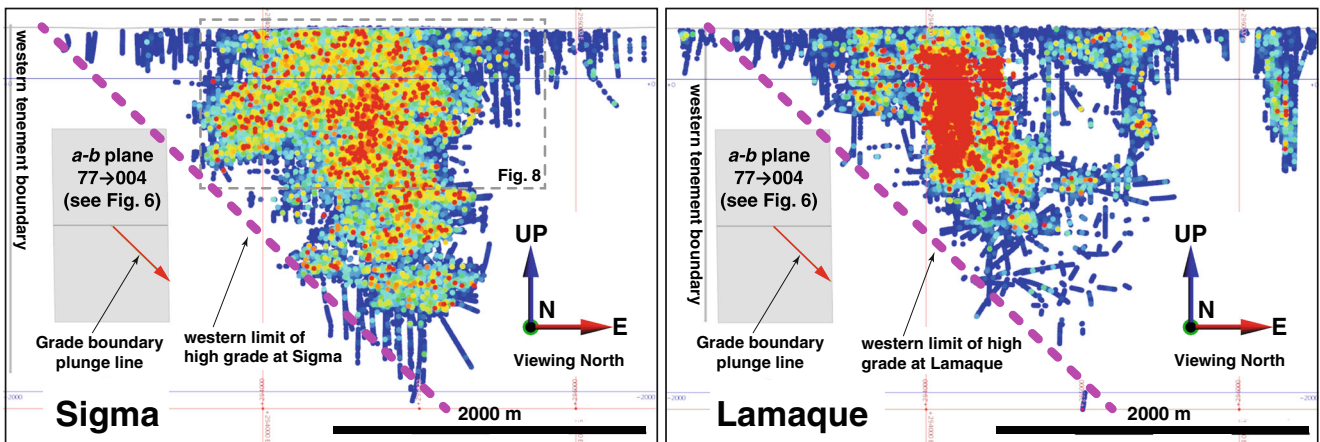
Fig. 9 Easterly-plunging western gold-grade limit at Sigma and Lamaque (dashed pink line). Grades are rendered with *Maximum Intensity Projection*, which projects the highest grade through the low-grade halo along the line parallel to view (Cowan 2014a). Position of Fig. 8 shown as dashed outline

indicates proximity to a fold hinge.

The Undifferentiated Tuff that are logged from the Sigma-Lamaque deposit display identifiable bedding traces when viewed in a 3D visualization software. A view in the down-dip direction of S_2, assumed to be dipping $77° \rightarrow 004°$, estimated from Robert and Brown (1986a: fig. 5b), is shown in Fig. 10b. In this near plan view, there is a 24° angular obliquity between the bedding trace in the Undifferentiated Tuff (green) and the S_2 trace. When viewed in vertical section, there is a similar degree of obliquity between the S_0 and S_2 traces viewed in the S_2 plane (Fig. 10c). When viewed looking $44° \rightarrow 081°$,

Fig. 10 Evidence of deposit-scale folding of the Undifferentiated Tuff identified in drill hole data. **a** Geological map of the Sigma-Lamaque deposit by Olivo et al. (2006: fig. 2), with annotations added to highlight bedding (S_0) and foliation trace (S_2). Undifferentiated Tuff (green) and Felsic Volcanic (orange). **b** Viewed down-dip along S_2. **c** Viewed in vertical section along strike of S_2. **d** Down-plunge direction of the intersection between S_2 and S_0. See Supplementary video file *ESM1.mp4* for an explanation
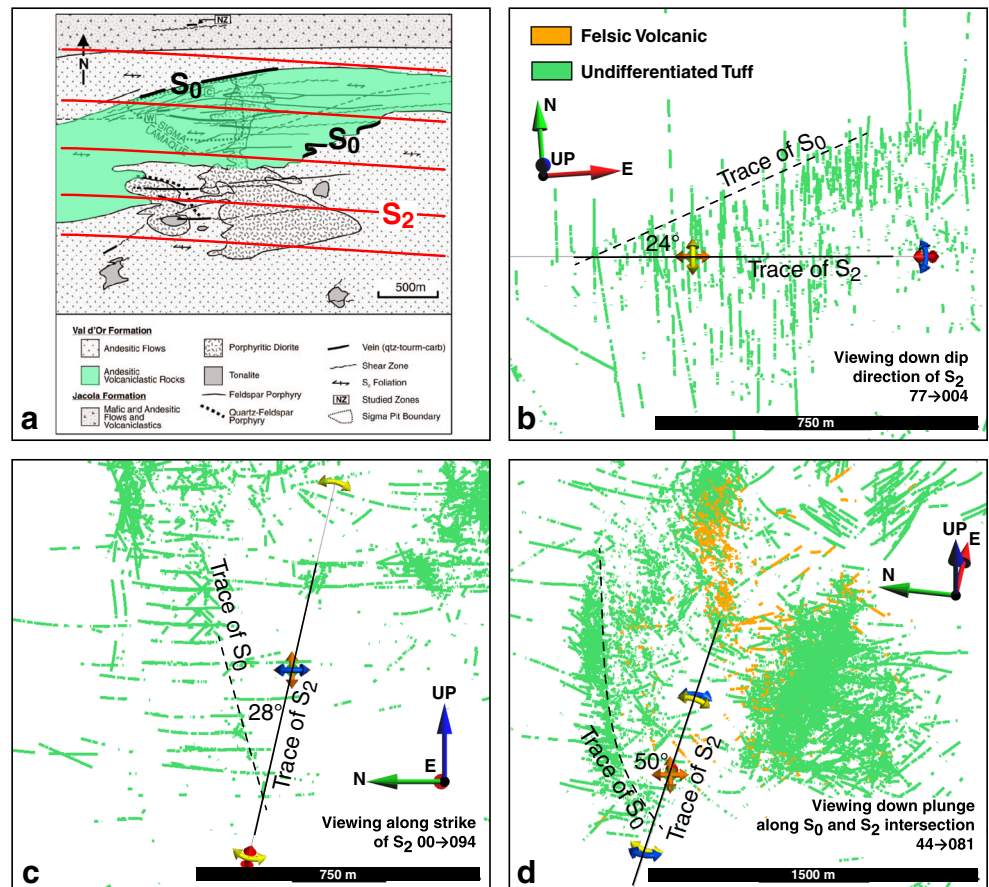
however, the intersection between S_0 and S_2 shows an obliquity of 50° (Fig. 10d). This is the largest possible obliquity angle between S_0 and S_2 and is evident when viewing in the S_2 plane and rotating the view about the pole of S_2. This view (Fig. 10d) equates with the down-plunge direction of the intersection between S_2 and S_0 (i.e., "down-structure" method of MacKin 1950). In this view, the trace of bedded units in the Undifferentiated Tuff (green) and Felsic Volcanic (orange) is evident in the Sigma side of the deposit (Fig. 10d).

All observations of the Sigma-Lamaque deposit listed above can be explained by a folded architecture of the Jacola and Val-d'Or Formations (Table 1). The a–b plane of the Late Diorite plugs (Fig. 6d) defines a planar orientation subparallel to S_2 ($77° \rightarrow 004°$) developed in the Jacola and Val-d'Or Formations, which has reported dips ranging from 70° to 90°, and dip-azimuth ranges from N–S to NNE–SSW (Claoué-Long et al. 1990; Morasse et al. 1995; Scott et al. 2002; Bedeaux et al. 2017).

The S_2-parallel orientation of the Late Diorites is consistent with syn- or post-fold emplacement into the axial planar region of a local asymmetrical F_2 fold closure during D_2. That is, the Late Diorites must have intruded along an existing planar heterogeneity in the country rock fabric, implying that the fabric *must have existed* before the diorite was emplaced. The fold axis is the region of highest structural dilation resulting from ductile and brittle strain. Metamorphic and/or igneous fluid flow and intrusions would focus along the plunge of the fold axis and by inference have the highest probability of localizing mineralization. This interpretation is consistent with the latest research on how granite melts are transported and emplaced in a compressive tectonic environment (Montanari et al. 2010; Ferré et al. 2012).

The angularity between the bedding (S_0) and tectonic foliation (S_2) defines an easterly plunge in the intersection line of these fabrics, and this expected fabric intersection plunge line that can be inferred from regional mapping (Fig. 2) coincides with the easterly plunge of the western grade boundary that is evident at Sigma-Lamaque (Fig. 9).

A 3D bedding-form surface model was constructed by interpolating bedding orientations (Vollgger et al. 2015)

Table 1 Observations (1 to 7) at Sigma-Lamaque explained in the context of folding strain of the Jacola and Val-d'Or Formations

| #	Observation	Explanation
1	Gold occurrence and lithology are dissimilar at Sigma and Lamaque	If fold-controlled structural permeability is the main control of mineralization, the gold distribution will largely be bedding parallel at the limb position and axial planar at the fold closure, which would transect the bedding. This explains the grade-lithology relationship contrast between Sigma and Lamaque, as Sigma is located in the fold limb position and Lamaque is located in the F_2 axial planar position.
2	Late Diorite plugs only exist at Lamaque	Lamaque Late Diorite plugs are located in a fold closure, which is commonly a zone of dilation compared to the fold limbs that tends to undergo layer-orthogonal compression. The low-grade zone between Sigma and Lamaque is parallel to S_2.
3	The Late Diorite plugs exhibit preferred orientation and geometry	The Lamaque Late Diorite plugs are located in the axial planar region of a F_2 parasitic fold and emplaced parallel to the S_2 foliation. The F_2 axial plane had the primary influence on its emplacement. This suggests that the Lamaque Late Diorite intrusions were emplaced during the end stages of D_2 deformation when F_2 had already formed. Temporal orientation of σ_2 to the vertical orientation emplaced the Late Diorites as subvertical linear plugs that are contained within the plane of S_2 foliation.
4	Vein orientations at Lamaque and Sigma display contrasting vein distributions	Fracture development and orientation depends on the attitude of the host rock anisotropy (Gomez-Rivas and Griera 2009) relative to the compression direction. Steep bedding in Sigma influenced development of misoriented reverse shear veins during high fluid pressure during an inferred to be N–S compression (Sibson et al. 1988). This resulted in vein development at Sigma that is highly asymmetric compared to the conjugate veins developed at Lamaque where bedding is interpreted to be less steep.
5	The Sigma-Lamaque vein swarms appear to converge at depth	Sigma veins are almost bedding-parallel, whereas Lamaque is axial-plane parallel; thus obliquity between these two areas is naturally expected in a fold closure setting.
6	The Sigma veins systematically shift orientation with position	Local stresses will be guided by local anisotropy (Dubé et al. 1989; Gomez-Rivas and Griera 2009), thus a spatial change in bedding orientation due to folding will change the vein development orientation to reflect this change in the underlying heterogenetic fabric.
7	An easterly plunging western grade boundary exists at both Sigma and Lamaque	This grade plunge is parallel to the fold plunge towards the east. The lower boundary to the grade is inferred to be a bedding layer within the Val-d'Or Formation, with poor permeability, which channeled the mineralized fluids upwards from its deeper source.
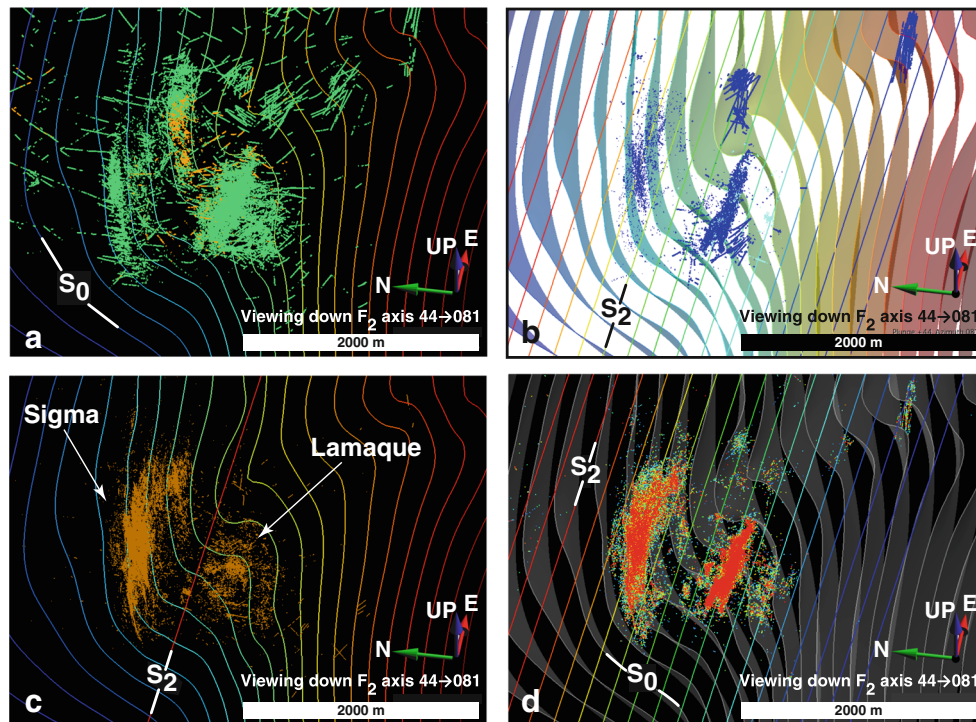
Fig. 11 F_2 fold model for Sigma-Lamaque. a Bedding trajectory traces with Undifferentiated Tuff (green) and Felsic Volcanic (orange) intervals. This view is in the same down-plunge direction as Figs. 10d and 13b. b Late Diorite (Early Quartz Diorite [navy] and Diorite [sky blue]) intervals show they are well developed parallel to S_2, but not along bedding at Lamaque. c Felsic to Intermediate Dykes (brown) distribution shows a clear boundary between Sigma and Lamaque. This low-grade boundary is interpreted from the magnetic data on the topography surface and the bedding traces visible in the drilling data when viewed in a 3D viewer (Fig. 11). The modeled bedding surfaces conform to the consistent southward younging of the Val-d'Or Formation, and are also consistent with the down-dip curvature of the bedding at depth visible in the logged lithologies at Sigma (Fig. 10d). Likely bedding traces can be identified in the magnetic data perturbations (reduced to pole, first vertical derivative, and horizontal gradient) and these were incorporated into the model (Fig. 12). No S_2 measurements were available, so a constant S_2 orientation of $77° \rightarrow 004°$ was assumed throughout the area of interest, with an F_2 fold plunge of $44° \rightarrow 081°$. The sections of Figs. 11 and 13b are viewed parallel to this F_2 plunge line.

parallel to S_2, as shown in red trace. This boundary was used to define the Sigma and Lamaque domains (Fig. 4). d Broadly bedding-parallel mineralization pattern in Sigma, and F_2 axial-plane parallel mineralization pattern at Lamaque. Only gold grades of ≥ 30 g/t shown in *Maximum Intensity Projection* rendering. See Supplementary video file *ESM3.mp4* for an explanation

The stereoplot in Fig. 13a summarizes the main structural orientations at Sigma-Lamaque. The Late Diorites are parallel to the S_2 fabric, but their linear axes have a steeper plunge than the plunge of F_2 (Fig. 13a, c). Their emplacement is likely to have been during protracted N–S shortening, but specifically when σ_2 switched with σ_3 into a near vertical position, with the Late Diorites intruded along σ_2 as prolate bodies parallel to the S_2 foliation plane. Interestingly, the plunge of the Late Diorites (Fig. 13a, c) is also subparallel to the steep NE-plunging stretching lineation L_2 developed in the Val-d'Or area, as reported by Bedeaux et al. (2017: figs. 13 and 16). This may indicate that the planar-linear geometry and orientation of the Late Diorites may have been influenced by pre-existing planar-linear schistosity S_2 developed during D_2.

Fracture development occurred when σ_2 reverted back to a horizontal E-W orientation after the emplacement of the Late Diorites (Fig. 7). Many quartz-tourmaline veins propagated outside the diorites to mineralize the adjacent lithological units in contact with the diorites. Because the brittle fracturing occurred after the major ductile deformation at the end of D_2 (Fig. 2) the competency of the diorite largely governed most of the fracture locations.

Supplementary video file *ESM1.mp4* displays the steps involved in identifying and working out the fold plunge from raw lithological data (Fig. 10), and how this plunge correlates to the western limit of the gold mineralization (Fig. 9). *ESM2.mp4* shows the spatial relationship of the mineralized

Fig. 12 3D bedding (S_0) and S_2 form surface model viewed in plan. **a** The modeled S_2 form surface traces at the topography surface are consistent with the grain in the horizontal gradient magnetic image. **b** The appearance of the 3D form surfaces of bedding (S_0) and S_2 below topography surface. Gold ≥ 30 g/t is shown as red dots. Positions of circular magnetic anomalies are shown and some correlate with Late Diorite plugs. See Supplementary video file *ESM2.mp4* for an explanation
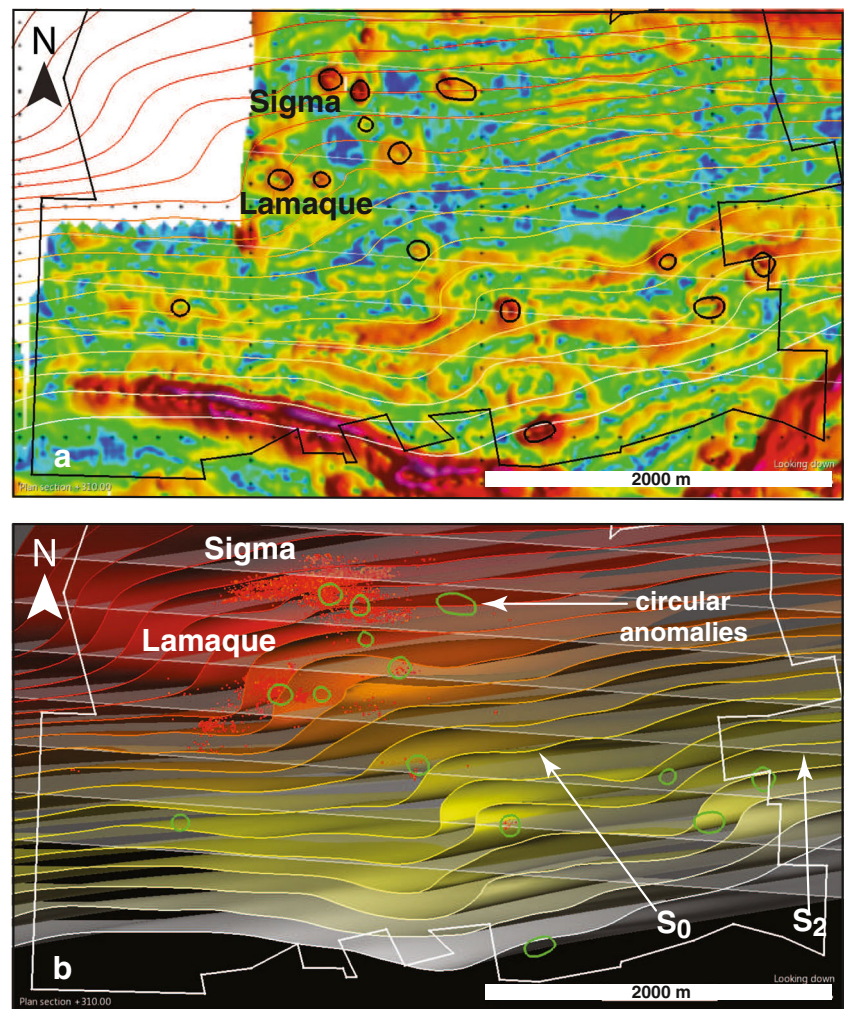
veins (Sigma and Lamaque stopes) to the F_2 fold plunge and the modeled folded stratigraphy.

Discussion

Comparison with previous work

The detailed descriptions of the vein systems developed at the Sigma mine in the original structural study of the Sigma deposit (Robert and Brown 1986a, b) and subsequent studies (e.g., Sibson et al. 1988; Robert and Poulsen 2001) have been influential in interpreting orogenic vein-hosted gold deposits as well as fluid flow research worldwide (e.g., Kontak et al. 1990; Cox et al. 1995; McCuaig and Kerrich 1998; Bierlein and Maher 2001; Cox and Ruming 2004; Dubé and Gosselin, 2007). At the time of Robert's research in the 1980s, the Lamaque deposit and the Sigma mine were owned by different companies and not all data could be accessed. However, a detailed description of the structural setting and the

characteristics of the gold-bearing veins of the Lamaque mine was previously described by Wilson (1948). This current study extends the analysis to the entire Sigma-Lamaque system and the observations and conclusions of Robert and Brown (1986a) are placed in the context of deposit-scale observations made from the entire gold deposit. Observation and analysis of a deposit's entire drilling data is now possible, some three decades since the seminal work of Robert (1983) and Sibson et al. (1988). In the intervening period, significant computer 3D rendering and processing methods have been developed, most importantly *Maximum Intensity Projection* (developed in 1989 [Wallis et al. 1989; Wikipedia contributors 2019]) and its application to analyze deposit-scale structural patterns from drill hole assay data (Cowan 2014a), and the introduction of implicit geological modeling software to the mining industry (Cowan et al. 2002, 2003; Cowan 2014b).

Largely based on Sigma's steep reverse and flat extensional vein systems that were described by Robert and Brown (1986a), Sibson et al. (1988) introduced the *fault-valve model*
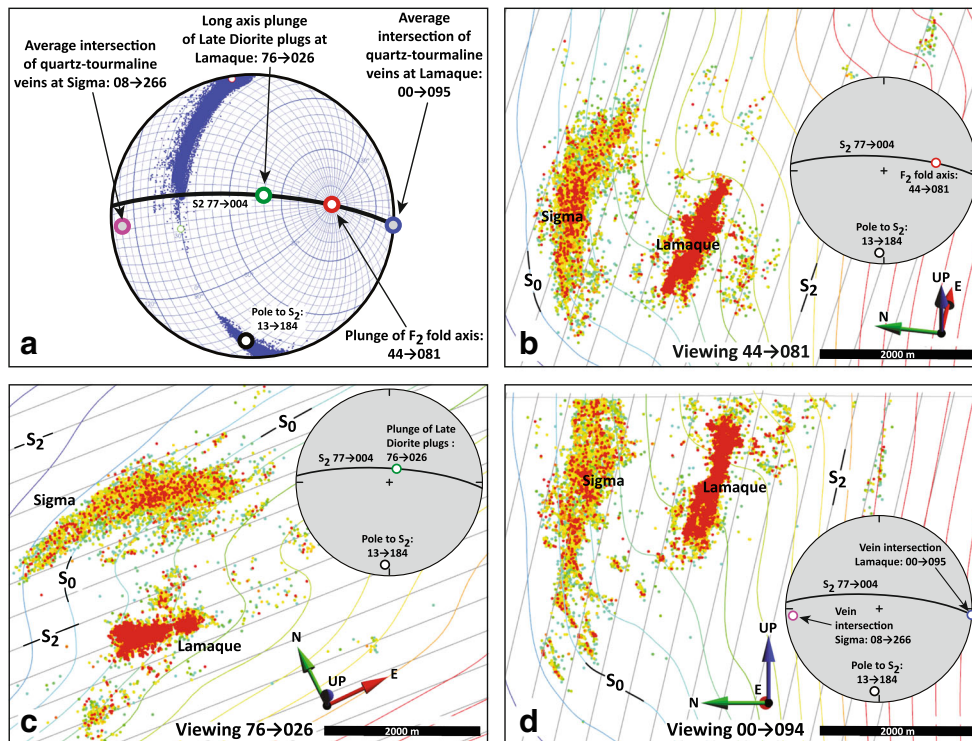
Fig. 13 D_2 structural elements of the Sigma-Lamaque deposit. **a** S_2 dips $77° → 004°$ and the F_2 fold axis plunges to $44° → 081°$. Lamaque Late Diorite plugs are parallel to S_2 but plunge more steeply than the F_2 fold axis. Intersections of the mineralized veins are subhorizontal and lie within S_2. Poles to the modeled bedding form surfaces (Fig. 12b) are shown in blue dots. Poles that plot in the south represent overturned south-facing bedding. **b** Gold grades (Au ≥ 30 g/t shown as red dots) with traces of 3D bedding (S_0 = colors) and S_2 (gray) form surface model viewed in F_2 down-plunge direction $44° → 081°$. This is the first-order mineralization continuity. **c** Same data with view parallel to the long axis (*a*-axis) of the Late Diorite plugs $76° → 026°$. This is the second-order mineralization continuity. **d** View horizontally along $00° → 094°$ in the S_2 plane and along the average intersections of all veins. This is the third-order mineralization continuity

of fault reactivation and accompanying ore fluid emplacement, a model further expounded by Sibson (1989, 1992) and Cox (1995, 2005, 2010). The fault-valve model called for high fluid pressure to account for the necessary lowering of the shearing strain along unfavorably oriented steep reverse faults that are at an unusually high angle (> 55°) to the maximum principal stress inferred from the subhorizontal extension veins. The existence of unexpected reverse shear veins, as opposed to thrusts that have a lower angle to the maximum principal stress, led Sibson et al. (1988) to conclude that the reactivation of the faults could only occur when fluid pressure exceeded the lithostatic load. Boullier and Robert (1992) provided microstructural evidence of cyclic growth and deformation in the veins from gold deposits in the Val-d'Or district and argued in support of the fault-valve model. The existence of unfavorably-oriented reverse shear veins is consistent evidence for high fluid pressure (Cox 2010), but the model does not explain why shear veins that are unfavorable in orientation initially formed, in preference to more favorable orientations, given

that high fluid pressure would influence the formation of veins of *any* orientation and kinematics (S.F. Cox, pers. comm., 2019). Under the presence of high fluid pressure, shear veins in favorable orientations would be expected to form, as recorded at Lamaque (Wilson 1948). However, at Sigma, only 500 m away, favorable shear vein orientations that dip south at a lower angle to the extension veins (< 55°) do not exist (Fig. 7b).

One possible explanation for the formation of the unfavorably oriented reverse shear veins at Sigma is that these veins are a small-scale expressions of a reactivated much larger "master shear zone" with prior history. Sibson et al. (1988) inferred that the small-displacement gold-bearing reverse shear veins at the Sigma mine, which are recorded down to 2 km, are part of a large brittle-ductile planar shear zone. This shear zone was interpreted to have a constant steep southerly dipping orientation that extended more than 10 km down into the base of the seismogenic zone where the Sigma deposit was interpreted to have been located. This interpretation was

reiterated further by Sibson (1989). The steep veins at Sigma were postulated to be parallel to a tabular shear zone that had an extent that was *five times* the vertical extent of drilling at Sigma mine. In other words, the 10 km vertical extent and the inferred constant steep orientation of the fault zone proposed by Sibson et al. (1988) is effectively the result of an "Inside-Out" interpretation workflow (as illustrated in Fig. 1) where small-scale field data are scaled up to infer a larger-scale structural feature on the assumption of scalability being valid (Pumpelly's Principle). This detail requires examination as the interpreted presence of a large-scale shear zone directly affects gold exploration at Sigma-Lamaque, and is also relevant to near-mine exploration at many other vein-hosted gold deposits. Although the evidence regarding the cyclic nature of vein formation due to repeated fluid pressure fluctuations may be consistent with the fault-valve model (Boullier and Robert 1992), the inference that the Sigma deposit is part of an extensive steep shear zone is inconsistent with the deposit-scale data described in this study. At the heart of this query is whether the formational mechanics, deduced from studying the outcrop-scale veins, can inform the working geologist of the exploration potential for the mineralized veins at the much larger deposit scale.

The problems of inferring the existence of a large-scale brittle-ductile reverse shear zone at Sigma are:

- The steep shear veins at the Sigma side of the Sigma-Lamaque gold deposit do not continue at the same dip along the total depth sampled and exhibit a lower dip at depths of 1500–2000 m (red traces in Fig. 14).
- Steep reverse shear veins do not continue along a steep southerly-dipping shear zone parallel to the shear veins as predicted by Sibson et al. (1988). The enveloping surface of the veins at Sigma was documented by Robert and Brown (1986a: fig. 3) and Sibson et al. (1998: fig. 1) to be vertical or dipping steeply to the north, and this is confirmed in this study (Fig. 14). This pattern contradicts the southerly-dipping reverse-shear model, but was not emphasized in the discussion by Sibson et al. (1988).
- The Sigma and Lamaque vein systems appear to converge at depth (Observation 5). This contradicts the tabular-planar shear plane geometry as represented by the Sigma set of veins as postulated by Sibson et al. (1988: fig. 2). Lamaque veins, which are the most productive gold-bearing veins in the Sigma-Lamaque system, exhibit an enveloping surface geometry that dips steeply north; therefore, these veins cannot be reconciled with a southerly-dipping reverse shear zone as proposed by Sibson et al. (1988).

- The North and South Shears, which are vertical with a thickness of 2 m on average and laterally extensive to 1 km both along strike and down-dip, as described by Robert and Brown (1986a), were not integrated into the model by Sibson et al. (1988). These shears, noted also by Gaboury et al. (2001), appear to be geologically significant, as they bound the vein development at Sigma. Although the positions of the North and South Shears were not provided by Integra Gold, these shears appear to be at the same orientation as the modeled bedding trace (Fig. 14) and could represent flexural slip planes along lithological or bedding contrasts that were active during the folding of the Val-d'Or Formation.
- In the plane-strain dip-slip shear model of Sibson et al. (1988), which was also reiterated by Robert et al. (1995), the gold distribution would be expected to exhibit the same symmetry as the mechanism proposed by Sibson et al. (1988). That is, the three-dimensional gold distribution at Sigma would exhibit the same symmetry as the proposed dip-slip mechanism (Patterson and Weiss 1961), so, in this scenario, the deposit-scale low-grade gold distribution would be expected to pitch down-dip parallel to the thrust movement along the proposed south-dipping reverse shear zone. Apparently supporting this prediction, Gaboury et al. (2001) noted that the mineralized envelope in the longitudinal section plunged parallel to the slip lineations measured within the Sigma reverse shear veins. In detail, however, the plunge illustrated by Gaboury et al. (2001: fig. 6) is at a smaller pitch angle than the large pitch angle expected from the measured slip lineations. The first-order long-range low-grade gold distribution at Sigma (as well as at Lamaque) pitches to the east at 45° (Fig. 9) and not 70° to 90° as expected, parallel to the measured slip lineations. This 3D pattern of gold distribution does not parallel the symmetry axes of the proposed dip-slip model of Sibson et al. (1988).
- In contrast to south-over-north shearing in a narrow reverse shear as proposed by Sibson et al. (1988), bulk north-over-south plane-strain non-coaxial shearing better explains the asymmetry in total vein occurrences at Sigma-Lamaque (Fig. 14, inset). The prevalence of south-dipping shear veins at both Sigma and Lamaque (Fig. 7b) implies that the line of extension plunged steeply to the north during veining, as opposed to vertical, which would result in a symmetrical vein distribution with equal occurrences of north and south-dipping shear veins. The line of extension during the formation of the veins is interpreted to be roughly in the plane of the north-dipping S_2 cleavage.
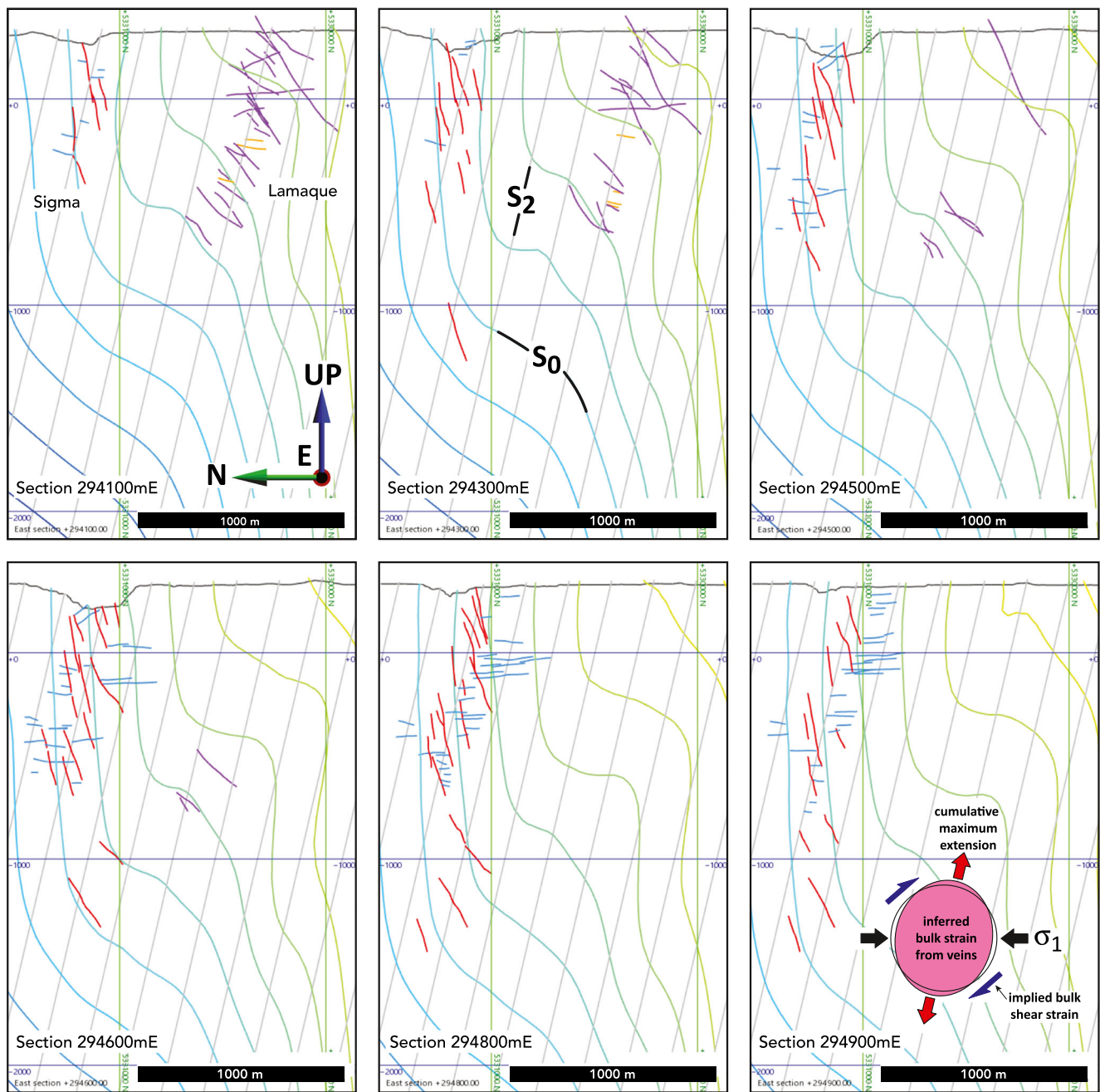
Fig. 14 Vertical section with view east showing the traces of Sigma shear veins (red) and horizontal extension veins (blue), and Lamaque conjugate shear veins (purple) and horizontal extension veins (orange). The colored contours are traces of the modeled bedding (S₀) form surfaces and the gray lines are S₂ form surface traces. Inferred extension is plunging steeply to the north, implied from the predominance of south-dipping shear veins. Together with the horizontal extension veins, this implies a north over though bulk shearing as schematically shown

Despite the argument for high fluid pressure in the formation of the vein systems at Sigma-Lamaque (Sibson et al. 1988), the knowledge of this mechanism itself cannot help determine the 3D geometry of the enveloping surfaces of these gold-bearing veins, which is the critical information required for within-mine and near-mine exploration in the district. The localization of high gold grades at the stope scale is parallel to the inferred σ_2 direction, which is horizontal and E–W (Fig. 7); therefore, this symmetry is consistent with the vein symmetry at Sigma-Lamaque. However, the gold distribution inferred by Sibson et al. (1988), from the kinematics of Sigma's south-dipping shear veins at stope scale, clearly cannot be scaled up to infer a deposit-scale gold distribution; neither can it predict the position of gold deposition over long

distances away from individual vein positions. As mentioned above, not only is gold distribution at Sigma steeply northerly-dipping instead of south-dipping, but the expected first-order plunge of the gold distribution is also inconsistent with the proposal of Sibson et al. (1988). This illustrates a fundamental shortcoming of applying the "Inside-Out" interpretation workflow by scaling up data at the outcrop scale.

Sibson (1996) concluded that the intermediate stress axis σ_2 is the axis of maximum structural permeability, but noted that the extent of this permeability "will depend on the 3D interconnectedness of the different structural elements." The vein patterns of the Sigma-Lamaque deposit clearly illustrate that the determination of the σ_2 direction from the orientation of stope-sized veins across the deposit (Fig. 7) is only relevant to the scale of the individual veins. That is, even if the measurements of vein orientations are obtained from across the sampled deposit, the inferred mean σ_2 direction cannot be used to extend the likely high-grade continuity hundreds of meters beyond the points of exposure because the extent of the vein swarms depend on the position of the *outer enveloping surface* of the vein swarm. The shape and continuity of the enveloping surface is the critical information required for ongoing within-mine exploration because it will affect the 3D interconnectedness of fluid flow (Sibson 1996). However, it is impossible to infer the vein swarm enveloping surface geometry from outcrop-scale observations of the veins or from vein orientation measurements. Instead, it requires a deposit-scale structural analytical approach by viewing and making structural sense of the entire mineralization pattern in 3D.

Nested hierarchical structural architecture

The 3D pattern of gold mineralization, and likely accompanying alteration envelope, at Sigma-Lamaque is a "nested" system with three orders of scale, each controlled by specific structural geological features. The gold continuity for each order can be truncated by the large-scale (lower-order) feature, and each order has its own structural symmetry that influences the grade continuity at that scale. The three orders of scale at Sigma-Lamaque are:

1. The first-order control is the zone of maximum dilation due to F_2 folding. For Sigma-Lamaque, it is the broad enveloping surface of the folded region in 3D (Fig. 12) and the mineralized volumes are bounded by local S_2 foliation and bedding (S_0). These mineralized zones plunge $44° \rightarrow 081°$ parallel to the intersection of S_0 and S_2 foliation (F_2 fold plunge) with the long-axis of the low-grade envelope parallel to this plunge line. This first-order control, where grade distribution is constrained in place by both S_0 and S_2, is obvious in the down-plunge

direction (Fig. 13b). However, the grade "continuities" are not continuous parallel to this plunge direction at every location, and highly mineralized volumes can transition to unmineralized zones along this plunge line. This is consistent with patterns recorded in other fold-hosted deposits (Newhouse 1942). It is largely determined by the structural permeability imposed by the foliation, bedding, lithology, and bedding-parallel faults that propagate from bedding surfaces. These are part of the first-order structural control, but are also affected by the second- and third-order controls that are nested within the first-order control.

2. The second-order control is provided by the geometry and position of the steeply plunging, structurally late, Late Diorite plugs, at Lamaque. The line of continuity of the second-order features, which are steeply plunging at Sigma-Lamaque, can be predicted, but the second-order continuity can be truncated or affected by the first-order controls of bedding (S_0) and laterally restricted by the S_2 foliation.

3. The third-order control is the geometry of the auriferous quartz-tourmaline veins that develop within the host rocks. These veins are not strictly confined to within the diorites, but there is a positive correlation (Fig. 5). Without close drill sampling, it is not possible to predict the exact positions of these veins. The vein orientation patterns of Sigma-Lamaque (Fig. 4) may be used to explore for local extensions to short distances, but vein swarms are predicted to be truncated by the second- and first-order controls (described above) that define the enveloping surface of the veins. The extents of the veins at Lamaque are laterally limited by the second-order control of the Late Diorite plugs, whereas the veins at Sigma are laterally limited by the first-order control of steep bedding (S_0) and S_2 foliation.

Supplementary video file *ESM3.mp4* shows how the high gold grade values in veins (third-order control) are laterally terminated by a combination of S_0 and S_2 foliation (first-order control). This animation also illustrates the bedding and Late Diorite plugs that parallel S_2 foliation.

Implications for orogenic gold mineralization and exploration

The greatest long-range exploration potential lies along the first-order trend, parallel to the F_2 fold plunge at Sigma-Lamaque. These first-order fold-controlled conduits are equivalent to the theoretical fluid pathways described in the mineral systems literature (fig. 3 in Knox-Robinson and Wyborn 1997). At Sigma-Lamaque, the plunging conduit radius is ~ 1.5 km

(Figs. 11d and 13b) and the drill-sampled mineralized down-plunge conduit length is ~ 3 km (Fig. 9). This conduit is interpreted to tap the lower crustal fluid source due to the plunging nature of the fold axis, and sporadic gold mineralization is predicted to exist in the down-plunge direction. Similar fold-controlled permeability pathways are possible at surface in the district surrounding the Sigma-Lamaque tenement within the folded Jacola and Val-d'Or Formations. Basic structural geological mapping using the traditional "Inside-Out" approach (Fig. 1), looking for angularity between bedding and S_2 foliation (Fig. 10a), is one way to locate similar fold-controlled pipe-like conduits where drilling data are unavailable. Where drilling data are available, the "Outside-In" workflow described in this study can be used to determine the first-order controls and thus potentially locate near-mine extensions to gold mineralization. However, locating a fold closure at surface may not necessarily lead to a discovery of gold mineralization there due to the possible presence of second-order controls down-plunge. Identifying a geochemical pathfinder and alteration anomaly expected at an outflow zone at surface is required before drilling to depth for possible mineralized pockets down-plunge (Beus and Grigorian 1977; Reis et al. 2001; Ord et al. 2012).

The first-order F_2 fold plunge trend, interpreted as the main pipe-like fluid conduit, is expected to be intersected internally by second-order controls; these are represented by the Late Diorite plugs at Sigma-Lamaque. These diorite plugs and other competent lithological units can be viewed as mineralization "traps", as discussed in mineral systems literature (Knox-Robinson and Wyborn 1997; McCuaig et al. 2010), which borrows terminology from petroleum systems literature that do not entirely apply to mineralization systems. More precisely, these fracture sites, formed in competent lithologies during late-orogenic compression (third-order control), feature the appropriate host composition to chemically react and precipitate gold from the fluid flowing along the first-order permeability pathway (Ord et al. 2012). Similar mineralization pockets hosted by diorite are predicted in the down-plunge direction of F_2. Late Diorite plugs are also expected in the district where there is well developed S_2 fabric, but the potential for gold mineralization may only occur if these bodies intersect with a first-order fluid conduit (Fig. 15). Supplementary video file *ESM4.mp4* explains the proposed Sigma-Lamaque F_2-paralell flow conduit model.

Despite the late-stage introduction of gold at Sigma-Lamaque, the distribution of the gold—as highlighted by the hierarchical arrangement of structural controls—is a function of the deformation history and resulting structural architecture. The structural architecture of the unmineralized rocks is critical to understanding the fluid pathway geometries—the structural patterns within these units offer the best clues to the geometric controls and the as yet undiscovered extensions of gold deposits.
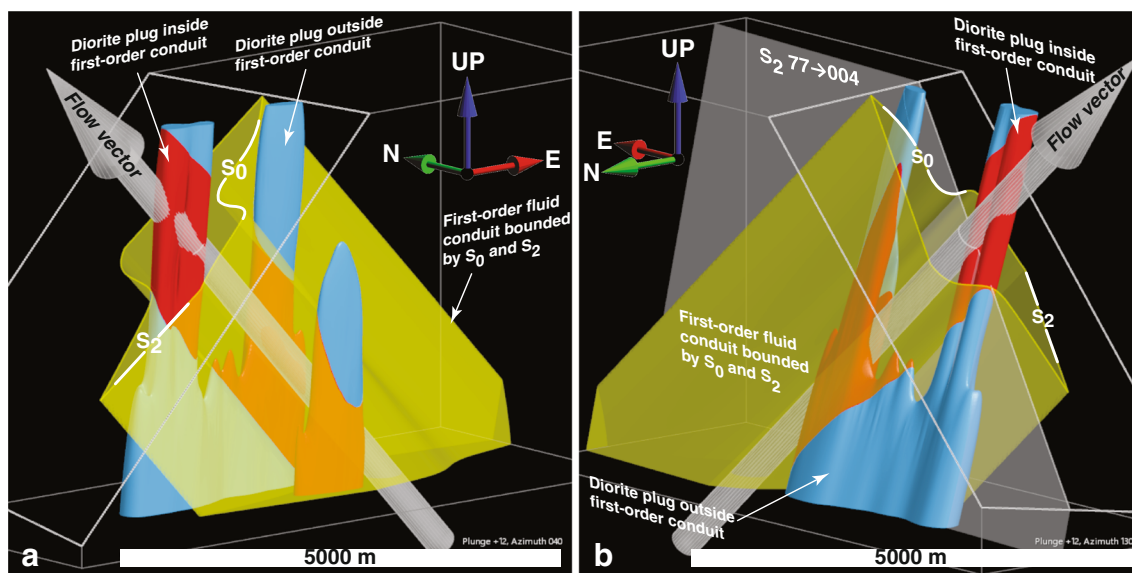

Fig. 15 Conceptual scaled block model of the Sigma-Lamaque fluid flow zone shown in cross-section orthogonal to F_2 plunge line (yellow). The first-order permeability zone is bounded by bedding S_0 and schistosity S_2 and upward direction of fluid flow indicated. The second-order Late Diorite plugs are intruded parallel to the S_2 fabric (red and blue solid). It is speculated that the portion of the plugs that intersect the fluid flow zone are more mineralized (red), compared to the parts of the intrusions which lie away from the flow envelope (blue). Much smaller third-order gold-bearing veins are not shown but they are limited laterally by the first- and second-order structures. **a** View towards $12° \rightarrow 040°$ and **b** view towards $12° \rightarrow 130°$ with orientation of S_2 shown. See Supplementary video file *ESM4.mp4* for an explanation

In orogenic gold systems in general, most effort should be placed on basic structural mapping that identifies the first-order controls in potential host rocks *away* from known mineralization, rather than be distracted with details of third-order features such as gold-bearing veins. It is not possible to work out the large-scale architecture controlling the fluid pathways that existed in orogenic gold systems from vein orientations alone (e.g., Fig. 7) because the more important vein-swarm-enveloping geometries are laterally limited by large-scale first- and second-order structural features.

Similarly, fine-resolution multi-parameter datasets obtained from drill cores cannot be used effectively in isolation without considering the large-scale structural architecture of the deposit. Current and future machine learning (ML) systems that maximize the knowledge gained from drill core data (Bérubé et al. 2018; Liu et al. 2019; Schnitzler et al. 2019) hold great promise for the minerals industry. Even though the benefits of ML are great, it is paramount that geologists know how to train these artificial computer algorithms to recognize large-scale hierarchical structural controls, otherwise ML systems may never yield sensible exploration targets.

Metamorphic vs magmatic-hydrothermal fluids debate

In the 1980s, a debate raged between researchers who saw Archean gold as originating from either metamorphic fluids (Phillips and Groves 1983; Groves et al.1987), or from syn-intrusion fluids (Burrows et al. 1986, Burrows and Spooner 1989). A groundbreaking study by Jemielita (1989) unequivocally established a ~90 million year time gap between the consolidation of Lamaque diorites (2685 ± 3 Ma, 2682 ± 2 Ma) and the quartz tourmaline veins that cross-cut and host the high-grade gold (2593 ± 5 Ma)(Fig. 3). Until that study, the relative timing of the intrusion and the gold-bearing veins was unclear. The veins could have been interpreted as roughly coeval with the consolidation of the Late Diorites, but the difference in nearly 100 million years was unexpected and significant, dispelling the igneous origin for gold (at least) at Lamaque. More studies followed that showed an unequivocal pattern of late-stage gold mineralization in the Abitibi Subprovince (Jemielita et al. 1990; Wong et al. 1991), and it is now generally recognized that gold mineralization globally occurred relatively late in the tectonic history of Archean greenstone belts (Groves et al. 1998, 2018; Dubé and Gosselin 2007; Ord et al. 2012).

Notwithstanding the apparent triumph of the metamorphic fluid theorists in the gold fluid origin debate 30 years' ago, this study raises an important structural geological relationship that was unrecognized until now—the plumbing system of the late-stage gold-bearing metamorphic fluids and igneous

intrusions may have been shared at Sigma-Lamaque during D_2 deformation, as manifested by the emplacement of the Late Diorite plugs parallel to S_2. This new interpretation legitimizes Spooner's intuition and research direction in the 1980s that was based on a critical geological observation—that gold occurrence and dioritic intrusions were spatially associated with each other in the Abitibi Subprovince (Burrows and Spooner 1989; Spooner 1993). The reason for this common occurrence appears to be the shared structural geological plumbing system between the metamorphic fluids and magmas and this has implications for other Archean orogenic terrains where there is co-spatial, but not necessarily co-temporal, occurrence of intrusions and gold (e.g., Allibone et al. 2004; Tourigny et al. 2018).

The fluid plumbing system at Sigma was previously interpreted to be a tabular crustal-scale shear zone (Sibson et al. 1988), and this view has had significant impact on the interpretation of orogenic gold deposits (Dubé and Gosselin 2007). However, the evidence from this study, in terms of considering both Sigma and Lamaque, favors a linear fold-controlled structural permeability pathway (fig. 9c in Sibson 1996). Folds with moderate to steep plunges have the potential to tap the deep source of these fluids and behave like linear pipe-like conduits. Injected parallel to S_2 foliation, the pathway followed by the Late Diorite plugs at depth is unknown. They may continue down-dip parallel to the S_2 foliation and coalesce into a single dyke as depicted in Fig. 15, or the plugs may follow parallel to the easterly F_2 plunge direction.

The abundance of gold deposits clustered along this boundary leaves little doubt that the Cadillac tectonic zone is a crustal-scale suture, which acted as a primary conduit for fluids (Rafini 2014). Therefore, researchers have focused primarily on the architecture and structural history of the Cadillac tectonic zone to explain the gold distribution along this suture (Robert et al. 1995; Bedeaux et al. 2017). But the Sigma-Lamaque deposit is 5 km from this boundary, and it is debatable whether the local brittle-ductile strains recorded there are from the distributed strain that resulted from the movement along the Cadillac tectonic zone. Furthermore, there are many more gold deposits in the region that are well away from the Cadillac tectonic zone (Fig. 2). The first-order 3D structural architecture of the host rocks examined at gold deposits distal from the Cadillac tectonic zone is likely to reveal important structural features that focused the fluid flow at each deposit location. It is postulated that the late orogenic gold-bearing fluids, which may or may not have been sourced from Cadillac tectonic zone, would have taken advantage of *any* structural permeability that had previously existed in the host rocks at shallower crustal levels. These structural pathways are not necessarily

associated with strains attributable to movements along the Cadillac tectonic zone.

Tectonic history during D_2 deformation

The structural controls defined in this study, together with previously published geochronological data, give a unique insight into the tectonic history of this part of the Abitibi Subprovince. The structural data presented in this study illustrate the remarkably simple relationships between the D_2 deformation architecture and the form of the Late Diorite intrusions at Lamaque, as well as the symmetry of the gold-bearing veins. Despite the implied temporary rotation of σ_2 to vertical during the Late Diorite plug emplacement, the σ_1 axis recorded by the veins at Sigma-Lamaque is virtually coaxial to the pole of S_2 (Figs. 7b and 14). This is significant because, if the tectonic history has a component of non-coaxial transcurrent strain in which stress and cumulative strain axes are not parallel to each other, there should be an appreciable angular difference between the pole of the cumulative strain fabric S_2 (or the minimum cumulative shortening axis λ_3) and the maximum stress axis σ_1 axis, determined from veins, which is an instantaneous record of strain (Fig. 7b). Due to the isotope ages established previously (Jemielita et al. 1989; Wong et al. 1991), the parallelism of σ_1 and λ_3 implies that there was little or no transcurrent deformation since the development of the S_2 fabric and the mineralized veins, which have a gap of ~90 Ma between them. Therefore, the interpretation that D_2 is transpressional (Robert 1989) may only relate to the earliest folding stages of D_2, but not the end stages after S_2 had developed and the mineralized quartz-tourmaline veins were formed at Sigma-Lamaque. The strain history suggests that the gold-bearing veins at Sigma-Lamaque formed during N–S shortening, with the only non-coaxiality seen in the vertical plane, which implies north-over-south plane-strain bulk deformation with subvertical extension (Fig. 14). This is consistent with the end stages of a long protracted history of D_2 that formed the La Motte Anticline (Fig. 2), with gold mineralization formed at the end stages with its distribution controlled by the structural architecture on the steep southern limb of this anticline.

Conclusions

Deposit-scale structural analysis is a powerful "Outside-In" method to decipher the geometric controls of mineral deposits using the most readily available 3D data—the drill-hole data.

It is powerful because:

1. It does not rely on collecting modern sophisticated empirical data, but works on the most unsophisticated single column assay data that is abundant and readily available from historical deposits.
2. By applying basic principles of structural analysis, it rapidly establishes the geometric controls at the deposit-scale, which is the most relevant scale for mineral exploration and Resource definition.
3. It identifies the various structural controls at different scales, which cannot be readily identified using the traditional "Inside-Out" method of applied structural analysis.
4. Structural features that are likely to be seen in outcrop can be predicted using the "Outside-In" method and the interpretation can be readily field tested.

The interpretation of the Sigma-Lamaque gold deposit, made entirely from a historical drilling database, is a model that can be readily field tested. As with any model that explains natural patterns, it will likely be revised or even eliminated in the future if better geological interpretations can explain the deposit-scale patterns. However, what is most useful about deposit-scale structural analysis are the lessons learned by repeating the interpretation process many times by analyzing data from mature mines and advanced exploration projects. With experience, geologists can notice repeated structural patterns in assay data, and these geometric patterns can help them predict how sparsely drilled deposits are likely to behave in space, thus minimizing exploration uncertainty in new exploration projects. When grade distributions are understood as structural geological patterns, rather than merely treated as geometrical envelopes for Resource estimation, the lessons learned from this practice will greatly minimize the risk of Resource write-downs. Resource envelopes will be understood in the context of structural architecture, and continuities of grade can be predicted by integrating structural geological understanding. Structural interpretation and determining the control of orogenic gold deposits using assay data is not only possible but might become a key strategy to move away from the over-reliance of theoretical structural models that have had little impact on gold exploration, as discussed by Vearncombe and Zelic (2015).

continuing discussions which are always very educational. This study, including the development costs of proprietary software *Orefind* used to analyze the data, and the payment of open access publication fee, was self-funded. Monash University is acknowledged for providing access to their online library.

References

Allibone A, Hayden P, Cameron G, Duku F (2004) Paleoproterozoic gold deposits hosted by albite- and carbonate-altered tonalite in the Chirano district, Ghana, West Africa. Econ Geol 99:479–497

Arne D, House E, Pontual S, Huntington J (2016) Hyperspectral interpretation of selected drill cores from orogenic gold deposits in central Victoria, Australia. Australian J Earth Sci 63:1003–1025

Bedeaux P, Pilote P, Daigneault R, Rafini S (2017) Synthesis of the structural evolution and associated gold mineralization of the Cadillac Fault, Abitibi, Canada. Ore Geol Rev 82:49–69

Bergqvist M, Landström E, Hansson A, Luth S (2019) Access to geological structures, density, minerals and textures through novel combination of 3D tomography, XRF and sample weight. Abstract volume of AEGC 2019: From data to discovery—Perth, Australia

Bérubé CL, Olivo GR, Chouteau M, Perrouty S, Shamsipour P, Enkin RJ, Feltrin L, Thiémonge R (2018) Predicting rock type and detecting hydrothermal alteration using machine learning and petrophysical properties of the Canadian Malartic ore and host rocks, Pontiac Subprovince, Québec, Canada. Ore Geol Rev 96:130–145

Beus AA, Grigorian SV (1977) In: Levinson AA (ed) Geochemical exploration methods for mineral deposits. Applied Publishing Ltd, Moscow, p 280

Bierlein FP, Maher S (2001) Orogenic disseminated gold in Phanerozoic fold belts—examples from Victoria, Australia and elsewhere. Ore Geol Rev 18:113–148

Boullier A-M, Robert F (1992) Paleoseismic events recorded in Archean gold–quartz vein networks, Val d'Or, Abitibi, Quebec, Canada. J Struct Geol 14:161–179

Burrows DR, Spooner ETC (1989) Relationships between Archean gold quartz vein-shear zone mineralization and igneous intrusions in the Val d'Or and Timmins areas, Abitibi subprovince, Canada. In: The Geology of Gold Deposits: The Perspective in 1988 (eds Keys RR, Ramsay WRH, Groves DI), Economic Geology Monograph 6:424–44. The Economic Geology Publishing Co.

Burrows DR, Wood PC, Spooner ETC (1986) Carbon isotope evidence for a magmatic origin for Archean gold quartz vein ore deposits. Nature 321:851–854

Claoué-Long JC, King RW, Kerrich R (1990) Archaean hydrothermal zircon in the Abitibi greenstone-belt: constraints on the timing of gold mineralisation. Earth Planet Sci Lett 98:109–128

Cowan EJ (2014a) X-ray plunge projection—understanding structural geology from grade data. Australian Institute of Mining and Metallurgy Monograph 30: Mineral Resource and Ore Reserve Estimation — The AusIMM Guide to Good Practice, 2nd edn: 207–220

Cowan EJ (2014b) Overview—geological interpretation and geological modelling. Australian Institute of Mining and Metallurgy Monograph 30: Mineral Resource and Ore Reserve Estimation — The AusIMM Guide to Good Practice, 2nd edn:137–143

Cowan EJ, Beatson RK, Fright WR, McLennan TJ, Mitchell TJ (2002) Rapid geological modelling. In: Vearncombe J (ed) Applied structural geology for mineral exploration and mining international symposium abstract volume. Aust Inst Geosci Bull 36:39–41

Cowan EJ, Beatson RK, Ross HJ, Fright WR, McLennan TJ, Evans TR, Carr JC, Lane RG, Bright DV, Gillman AJ, Oshust PA, Titley M (2003) Practical implicit geological modelling. In: Dominy S (ed) Fifth International Mining Geology Conference Proceedings, Australasian Institute of Mining and Metallurgy Publication Series No 8, pp 89–99

Cowan EJ, Lane RG, Ross HJ (2004) Leapfrog's implicit drawing tool: a new way of drawing geological objects of any shape rapidly in 3D. In: Berry MJ, Quigley ML (eds) Mining Geology 2004 Workshop. Aust Inst Geosci Bull 41:23–25

Cox SF (1995) Faulting processes at high fluid pressures–an example of fault valve behavior from the Wattle Gully fault Victoria, Australia. J Geophys Res 100:12841–12859

Cox SF (2005) Coupling between deformation, fluid pressures, and fluid flow in ore-producing hydrothermal systems at depth in the crust. In: Hedenquist JW, Thompson JFH, Goldfarb RJ, Richards JP (eds) Economic Geology one hundredth anniversary volume 1905–2005. Society of Economic Geologists Inc, Littleton, Colorado, pp 39–75

Cox SF (2010) The application of failure mode diagrams for exploring the roles of fluid pressure and stress states in controlling styles of fracture-controlled permeability enhancement in faults and shear zones. Geofluids 10:217–233

Cox SF, Ruming K (2004) The St Ives mesothermal gold system, Western Australia—a case of golden aftershocks? J Struct Geol 26:1109–1125

Cox SF, Sun SS, Etheridge MA, Wall VJ, Potter TF (1995) Structural and geochemical controls on the development of turbidite-hosted gold quartz vein deposits, Wattle Gully mine, central Victoria, Australia. Econ Geol 90:1722–1746

Desrochers J-P, Hubert C (1996) Structural evolution and early accretion of the Archean Malartic Composite Block, southern Abitibi greenstone belt, Quebec, Canada. Can J Earth Sci 33:1556–1569

Dubé B, Gosselin P (2007) Greenstone-hosted quartz–carbonate vein deposits. In: Goodfellow WD (ed) Mineral deposits of Canada: a synthesis of major deposit-types, district metallogeny, the evolution of geological provinces, and exploration methods. Geological Association of Canada, Mineral Deposits Division, Special Publication 5: pp 49–73

Dubé B, Poulsen H, Guha J (1989) The effects of layer anisotropy on auriferous shear zones; the Norbeau Mine, Quebec. Econ Geol 84:871–878

Ferré EC, Galland O, Montanari D, Kalakay TJ (2012) Granite magma migration and emplacement along thrusts. Int J Earth Sci 101:1673–1688

Flinn D (1962) On folding during three-dimensional progressive deformation. Q J Geol Soc Lond 118:385–428

Gaboury D, Carrier A, Crevier M, Pelletier C, Sketchley DA (2001) Predictive distribution of fault-fill and extensional veins: example from the Sigma Gold Mine, Abitibi subprovince, Canada. Econ Geol 96:1397–1405

Garofalo P (2004) Mass transfer during gold precipitation within a vertically extensive vein network (Sigma deposit – Abitibi greenstone belt – Canada). Pt I. Patterns of hydrothermal alteration haloes. Eur J Mineral 16:753–760

Garofalo P, Matthäi SK, Heinrich CA (2002) Three-dimensional geometry, ore distribution and time-integrated mass transfer through the quartz–tourmaline–gold vein network of the sigma deposit (Abitibi belt, Canada). Geofluids 2:217–232

Gomez-Rivas E, Griera A (2009) Influence of mechanical anisotropy on shear fracture development. Trab Geol 29:305–311

Groves DI, Phillips GN, Ho SE, Houstoun SM, Standing CA (1987) Craton-scale distribution of Archean greenstone gold deposits: predictive capacity of the metamorphic model. Econ Geol 82:2045–2058

Groves DI, Goldfarb RJ, Gebre-Mariam M, Hagemann SG, Robert F (1998) Orogenic gold deposits-a proposed classification in the context of their crustal distribution and relationship to other gold deposit types. Ore Geol Rev 13:7–27

Groves DI, Santosh M, Goldfarb RJ, Zhang L (2018) Structural geometry of orogenic gold deposits: implications for exploration of world-class and giant deposits. Geosci Front 9:1163–1177

Haest M, Cudahy T, Laukamp C, Gregory S (2012a) Quantitative mineralogy from infrared spectroscopic data, Part I. Validation of mineral abundance and composition scripts at the Rocklea Channel Iron Deposit in Western Australia. Econ Geol 107:209–228

Haest M, Cudahy T, Laukamp C, Gregory S (2012b) Quantitative mineralogy from infrared spectroscopic data. Part II. Three-dimensional mineralogical characterization of the Rocklea Channel Iron Deposit, Western Australia. Econ Geol 107:229–249

Hanes JA, Archibald DA, Hodgson CJ, Robert F (1989) Preliminary 40Ar/39Ar geochronology and timing of Archean gold mineralization at the Sigma Mine, Val d'Or, Quebec, Curr Res Part C, Geol Surv Can, Paper 89–1C:135–142

Imreh L (1982) Sillon de La Motte-Vassan et son avant-pays meridional: Synthèse volcanologique, lithostratigraphique et gîtologique. Quebec Ministère de L'Energie et des Ressources, MM 82–04

Integra Gold Corp (2015). Integra Gold Rush Challenge. https://www.herox.com/IntegraGoldRush/community. Accessed 12 December 2019

Jemielita RA, Davis DW, Krogh TE, Spooner ETC (1989) Chronological constraints on the origin of Archaean lode gold deposits in the southern Superior Province from U-Pb isotopic analyses of hydrothermal rutile and sphene. Geol Soc Am, Abstr With Programs 21:6, pA351

Jemielita RA, Davis DW, Krogh TE (1990) U-Pb evidence for Abitibi gold mineralization postdating greenstone magmatism and metamorphism. Nature 346:831–834

Knox-Robinson CM, Wyborn LAI (1997) Towards a holistic exploration strategy: using geographic information systems as a tool to enhance exploration. Aust J Earth Sci 44:453–463

Kontak DJ, Smith PK, Kerrich R, Williams PF (1990) Integrated model for Meguma Group lode gold deposits, Nova Scotia, Canada. Geology 18:238–242

Liu J, Chen W, Chalup S, Wheeler C (2019) An automatic HyLogger(TM) mineral mapping method using a machine-learning-based computer vision technique. Aust J Earth Sci 66:1063–1073

MacKin JH (1950) Studies for Students: the down-structure method of viewing geological maps. J Geol 58:55–72

McCuaig TC, Kerrich R (1998) P—T—t—deformation—fluid characteristics of lode gold deposits: evidence from alteration systematics. Ore Geol Rev 12:381–453

McCuaig TC, Beresford S, Hronsky J (2010) Translating the mineral systems approach into an effective exploration targeting system. Ore Geol Rev 38:128–138

Montanari D, Corti G, Sani F, Del Ventisette C, Bonin M, Moratti G (2010) Experimental investigation on granite emplacement during shortening. Tectonophysics 484:147–155

Morasse S, Wasteneys HA, Cormier M, Helmstaedt H, Mason R (1995) A pre-2686 Ma intrusion-related gold deposit at the Kiena Mine, Val d'Or, Quebec, Southern Abitibi Subprovince. Econ Geol 90:1310–1321

Newhouse WH (1942) Structural featured associated with the ore deposits described in this volume. In: Newhouse WH (ed) Structural features associated with the ore deposits: ore deposits as related to structural features. Princeton University Press, New Jersey, pp 9–53

Olivo GR, Chang F, Kyser TK (2006) Formation of the auriferous and barren North Dipper veins in the Sigma Mine, Val d'Or, Canada: constraints from structural, mineralogical, fluid inclusion, and isotopic data. Econ Geol 101:607–631

Ord A, Hobbs BE, Lester DR (2012) The mechanics of hydrothermal systems: I. Ore systems as chemical reactors. Ore Geol Rev 49:1–44

Patterson MS, Weiss LE (1961) Symmetry concepts in the structural analysis of deformed rocks. Geol Soc Am Bull 72:841–882

Perrault G, Trudel P, Bedard P (1984) Auriferous halos associated with the gold deposits at Lamaque mine, Quebec. Econ Geol 79:227–238

Phillips GN (ed) (2017) Australian Ore Deposits. Melbourne, The Australian Institute of Mining and Metallrgy, p 864

Pilote P (2015a) Geology – Val d'Or. Quebec MERN Map CG-32C04A-2015-01, 1:20 000 scale

Pilote P (2015b) Geology – Lake Montigny. Quebec MERN Map CG-32C04C-2015-01, 1:20 000 scale

Poirier S, Roy L, D'Amours C, Gaudreault D, Bergeron S, Ilieva T, Utiger M (2015a) Technical report and mineral resource estimate update for the Lamaque project (according to National Instrument 43-101 and Form 43-101F1), Bourlamaque Township. Technical report prepared by InnovExplo for Integra Gold Corp, Province of Québec, Canada

Poirier S, Roy L, D'Amours C, Gaudreault D, Bergeron S, Ilieva T, Utiger M (2015b) Technical report and updated preliminary economic assessment for the Lamaque project (according to National Instrument 43-101 and Form 43-101F1), Bourlamaque Township. Technical report prepared by InnovExplo for Integra Gold Corp, Province of Québec, Canada

Financial Post (2016) Rubicon Minerals Corp shares plunge as miner slashes its gold resources by 88%. http://business.financialpost.com/news/mining/rubicon-minerals-corp-shares-plunge-as-miner-slashes-its-gold-resources-by-88. Accessed 12 December 2019

Financial Post (2019) 'The gold was never there': A miner's reserves evaporate amid battle with former CEO https://business.financialpost.com/commodities/mining/the-gold-was-never-there-a-miners-reserves-evaporate-amid-battle-with-former-ceo. Accessed 12 December 2019

Pumpelly R, Wolff JE, Dale TN (1894) The geology of the Green Mountains. US Geol Surv Mem 23:1–157

Rafini S (2014) Typologie des minéralisations aurifères associées a la faille de Cadillac. Rapport du projet CONSOREM 2011-01 et 2012-01, 45p. http://www.consorem.ca/production_scientifique/2012_01/2012-01_Gitologie%20Faille%20Cadillac_FINAL.pdf. Accessed 12 December 2019

Reis AP, Sousa AJ, Cardoso Fonseca E (2001) Soil geochemical prospecting for gold at Marrancos (northern Portugal). J Geochem Explor 73:1–10

Robert F (1983) Etude du mode de mise en place des veines aurifères de la mine Sigma, Val d'Or, Québec. Unpubl PhD. thesis, Ecole Polytechnique, University of Montréal

Robert F (1989) Internal structure of the Cadillac tectonic zone southeast of Val d'Or, Abitibi greenstone belt, Quebec. Can J Earth Sci 26:2661–2675

Robert F, Brown AC (1986a) Archean gold-bearing quartz veins at the Sigma Mine, Abitibi greenstone belt, Quebec; part I, geologic relations and formation of the vein system. Econ Geol 81:578–592

Robert F, Brown AC (1986b) Archean gold-bearing quartz veins at the Sigma Mine, Abitibi greenstone belt, Quebec; part II, vein paragenesis and hydrothermal alteration. Econ Geol 81:593–616

Robert F, Poulsen KH (1997) World-class Archaean gold deposits in Canada: an overview. Aust J Earth Sci 44:329–351

Robert F, Poulsen KH (2001) Vein formation and deformation in greenstone gold deposits. Soc Econ Geol Rev 14:111–155

Robert F, Boullier A-M, Firdaous K (1995) Gold-quartz veins in metamorphic terranes and their bearing on the role of fluids in faulting. J Geophys Res 100:12861–12879

Schnitzler N, Ross P-S, Gloaguen E. (2019) Using machine learning to estimate a key missing geochemical variable in mining exploration: application of the Random Forest algorithm to multi-sensor core logging data. J Geochem Explor 205: (in press)

Schodlok MC, Whitbourne L, Huntington J, Mason P, Green A, Berman M, Coward D, Connor P, Wright W, Jolivet M, Martinez R (2016) HyLogger-3, a visible to shortwave and thermal infrared reflectance spectrometer system for drill core logging: functional description. Australian J Earth Sci 63:929–940

Scott CR, Mueller WU, Pilote P (2002) Physical volcanology, stratigraphy, and lithogeochemistry of an Archean volcanic arc: evolution from plume related volcanism to arc rifting of SE Abitibi greenstone belt, Val d'Or, Canada. Precambrian Res 115:223–260

Sibson RH (1989) Earthquake faulting as a structural process. J Struct Geol 11:1–14

Sibson RH (1992) Implications of fault-valve behavior for rupture nucleation and recurrence. Tectonophysics 211:283–293

Sibson RH (1996) Structural permeability of fluid-driven fault-fracture meshes. J Struct Geol 18:1031–1042

Sibson RH, Robert F, Poulsen H (1988) High-angle reverse faults, fluid-pressure cycling, and mesothermal gold-quartz deposits. Geology 16:551–555

Sjöqvist ASL, Lundström A, Artursson M (2017) Minalyzer CS: Rapid, non-destructive, on-site assaying of drilling samples. Exploration '17 Sixth Decennial International Conference on Mineral Exploration, Workshop 9 – Status and New Developments in Field Portable Geochemical Techniques and Site Technologies for Mineral Exploration, Toronto, Canada, October 26th, 2017

Spooner ETC (1993) Magmatic sulphide/volatile interaction as a mechanism for producing chalcophile element enriched, Archean Au-quartz, epithermal Au-Ag and Au skarn hydrothermal ore fluids. Ore Geol Rev 7:359–379

Tourigny G, Masurel DT, Masurel Q, Kreuzer O, Brammer S, Owusu-Ansah K, Yao D, Heyford T (2018) Structural controls on granitoid-hosted gold mineralization and paleostress history of the Edikan gold deposits, Kumasi Basin, southwestern Ghana. Mineral Deposita 54:1033–1052

Tremblay A (2001) Postmineralization faults in the Beaufor Gold Deposit, Abitibi greenstone belt, Canada: geometry, origin, and tectonic implications for the Val d'Or mining district. Econ Geol 96:509–524

Van Hise CR (1896) Studies for Students: deformation of rocks.: II. An analysis of folds. J Geol 4:312–353

Vearncombe J, Zelic M (2015) Structural paradigms for gold: do they help us find and mine? App Earth Sci Trans Inst Min Metall Sect B 124:2–19

Vollgger SA, Cruden AR, Ailleres L, Cowan EJ (2015) Regional dome evolution and its control on ore-grade distribution: insights from 3D implicit modelling of the Navachab gold deposit, Namibia. Ore Geol Rev 69:268–284

Wallis JW, Miller TR, Lerner CA, Kleerup EC (1989) Three dimensional display in nuclear medicine. IEEE Trans Med Imaging 8:297–303

Wikipedia contributors (2019) Maximum intensity projection, Wikipedia, the Free Encyclopedia [online] http:// enwikipediaorg/wiki/Maximum_intensity_projection Accessed 12 December 2019

Wilde A, Kreuzer O (2016) The role of crowdsourcing in gold exploration. AIG News 124:38–43

Wilson HS (1948) Lamaque Mine. In: Structural geology of Canadian ore deposits: a symposium arranged by a Committee of the Geology Division. Canadian Institute of Mining and Metallurgy, Montreal, pp 882–891

Wong L, Davis DW, Krogh TE, Robert F (1991) U–Pb zircon and rutile chronology of Archean greenstone formation and gold mineralization in the Val d'Or region, Quebec. Earth Planet Sci Lett 104:325–336

Springer